

Development of Platinum-copper Core-shell Nanocatalyst on Multi-Walled  
Carbon Nanotubes for Proton Exchange Membrane Fuel Cells

by

Anthony Adame

A Thesis Presented in Partial Fulfillment  
of the Requirements for the Degree  
Master of Science in Technology

Approved April 2012 by the  
Graduate Supervisory Committee:

Arunachalanadar Madakannan, Chair  
Xihong Peng  
Govindasamy Tamizhmani

ARIZONA STATE UNIVERSITY

May 2012

## ABSTRACT

With a recent shift to a more environmentally conscious society, low-carbon and non-carbon producing energy production methods are being investigated and applied all over the world. Of these methods, fuel cells show great potential for clean energy production. A fuel cell is an electrochemical energy conversion device which directly converts chemical energy into electrical energy. Proton exchange membrane fuel cells (PEMFCs) are a highly researched energy source for automotive and stationary power applications. In order to produce the power required to meet Department of Energy requirements, platinum (Pt) must be used as a catalyst material in PEMFCs. Platinum, however, is very expensive and extensive research is being conducted to develop ways to reduce the amount of platinum used in PEMFCs.

In the current study, three catalyst synthesis techniques were investigated and evaluated on their effectiveness to produce platinum-on copper (Pt@Cu) core-shell nanocatalyst on multi-walled carbon nanotube (MWCNT) support material. These three methods were direct deposition method, two-phase surfactant method, and single-phase surfactant method, in which direct deposition did not use a surfactant for particle size control and the surfactant methods did. The catalyst materials synthesized were evaluated by visual inspection and fuel cell performance. Samples which produced high fuel cell power output were evaluated using transmission electron microscopy (TEM) imaging.

After evaluation, it was concluded that the direct deposition technique was effective in synthesizing Pt@Cu core-shell nanocatalyst on MWCNTs support

when a rinsing process was used before adding platinum. The peak power density achieved by the rinsed core-shell catalyst was  $618 \text{ mW}\cdot\text{cm}^{-2}$ , 13 percent greater than that of commercial platinum-carbon (Pt/C) catalyst. Transmission electron microscopy imaging revealed the core-shell catalyst contained Pt shells and platinum-copper alloy cores. Rinsing with deionized (DI) water was shown to be a crucial step in core-shell catalyst deposition as it reduced the number of platinum colloids on the carbon nanotube surface.

After evaluation, it was concluded that the two-phase surfactant and single-phase surfactant synthesis methods were not effective at producing core-shell nanocatalyst with the parameters investigated.

## DEDICATION

To my parents  
Oscar and Rita Adame

## ACKNOWLEDGMENTS

I would first like to express my deepest gratitude to my graduate committee chair and research advisor, Dr. Arunachalanadar Madakannan, for his guidance and support that will affect me for the rest of my life. I thank him for patiently guiding me through the research process, allowing me to grow not only in academia, but in my personal life as well.

I am grateful to my thesis committee member, Dr. Xihong Peng for her dedication and guidance throughout my thesis work and for her time meeting with me to keep me on track.

I am grateful to my thesis committee member, Dr. Govindasamy Tamihzmani for his dedication and commendable guidance throughout my thesis work.

I am grateful to Dr. Thomas Dory for his help discussing my work and for help with chemistry concepts.

I would like to thank my colleague, research advisor, and friend, Jiefeng Lin, for his invaluable guidance and support during my studies and thesis work. His contributions are treasured and will never be forgotten.

I would like to thank my colleagues and friends, Rashida Villacorta, Eric Hinkson, Qurat-ul-ain Shah, Aditi Jhalani, Xuan Liu, Adam Arvay, Eric Berger, Yen Huang, Chad Mason, Kartik Kinhal, and Brian Fauss for their support and encouragement throughout my thesis work.

Transmission electron microscopy was conducted by Karl Weiss of the LeRoy Eyring Center for Solid State Science at Arizona State University and is greatly acknowledged.

I would like to thank Rene Fischer and Cheryl Roberts for assistance in ordering supplies as well as Scott McAdams and Robert Sandoval for the use of equipment. I also would like to thank Julie Barnes and Martha Benton for help with fellowship questions and scheduling of the thesis defense.

I would not have embarked on this journey had it not been for the ASU/NASA Space Grant Program. I would like to thank Dr. Thomas Sharp and Candace Jackson for their support during my time as a Space Grant Intern which led to this research.

I am also very thankful to the donors of the Security and Defense Systems Initiative Fellowship for their financial assistance which helped me focus more of my time on this research.

Lastly, I would like to thank the people that have been there for me the most and that I could not thank enough. I would like to thank my friends for their continued support of my education and my happiness. I would like thank my family for their heartwarming words of encouragement when I needed it the most. I would like to especially thank my loving girlfriend, Alena Caravetta, for being a pillar of strength and support and for her ability to always know the right things to say to make me feel better when I feel stressed or frustrated.

I would most importantly like to thank my parents, Oscar and Rita, who have always supported my education and have taught me by example to work

hard and take pride in my work. They have been great teachers and I could not ask for better guidance than what has been provided by them. Their enduring kindness and love is the fuel that keeps me going forward in my success.

## TABLE OF CONTENTS

	Page
LIST OF TABLES.....	xi
LIST OF FIGURES.....	xii
CHAPTER	
1 INTRODUCTION.....	1
1.1 Background.....	1
1.2 Statement of problem .....	5
1.3 Scope of work .....	7
1.4 Organization of thesis.....	7
2 LITERATURE REVIEW .....	9
2.1 Fuel cell history .....	9
2.2 Technical challenges for fuel cells.....	9
2.2.1 Cost .....	10
2.2.2 Durability.....	10
2.2.3 Performance.....	11
2.3 Fuel cell electrical losses .....	12
2.4 Electrocatalyst support materials .....	14
2.5 Functionalization of multi-walled carbon nanotubes .....	15
2.6 Surfactant materials .....	16
2.7 Core-shell nanoparticles .....	18
3 METHODOLOGY.....	21



CHAPTER	Page
3.1 Materials used .....	21
3.2 Experimental methods .....	21
3.3 Experimental setup .....	22
3.4 pH control of copper sulfate solution.....	23
3.5 Fuel cell fabrication .....	23
3.6 Cyclic voltammetry and fuel cell testing .....	25
4 DIRECT DEPOSITION METHOD .....	27
4.1 Experimental details .....	27
4.1.1 Fabrication methodology .....	27
4.1.2 Functionalization of carbon nanotubes .....	27
4.1.3 Preparation of copper sulfate solution .....	27
4.1.4 Reduction methods .....	28
4.1.5 Evaluation of reaction .....	30
4.1.6 Rinsing and galvanic displacement.....	30
4.1.7 Filtering and washing .....	31
4.1.8 Acid treatment .....	31
4.1.9 Cyclic voltammetry activation.....	31
4.1.10 Summary of process steps.....	31
4.1.11 Theoretical nanoparticle structure.....	34
4.1.12 Characterization.....	34
4.2 Results and discussion .....	35
4.2.1 Chemical reduction .....	35

CHAPTER	Page
4.2.2 Fuel cell test results .....	37
4.2.3 Microscopic imaging.....	39
5 TWO-PHASE SURFACTANT METHOD .....	48
5.1 Experimental methods .....	48
5.1.1 Fabrication methodology .....	48
5.1.2 Functionalization of carbon nanotubes .....	48
5.1.3 Preparation of copper sulfate solution .....	49
5.1.4 Copper reduction .....	49
5.1.5 Filtering and heat treatment .....	49
5.1.6 Galvanic displacement .....	49
5.1.7 Filtering and washing .....	51
5.1.8 Acid treatment .....	51
5.1.9 Cyclic voltammetry and fuel cell testing .....	51
5.1.10 Summary of process steps.....	51
5.1.11 Theoretical nanoparticle structure.....	53
5.2 Results and discussion .....	54
5.2.1 Chemical reduction .....	54
5.2.2 Galvanic displacement .....	55
5.2.3 Fuel cell output .....	55
6 SINGLE-PHASE SURFACTANT METHOD .....	57
6.1 Experimental details .....	57
6.1.1 Fabrication methodology .....	57

CHAPTER	Page
6.1.2 Functionalization of carbon nanotubes .....	57
6.1.3 Preparation of copper sulfate solution .....	58
6.1.4 Copper reduction .....	58
6.1.5 Rinsing with DI water .....	58
6.1.6 Galvanic displacement .....	58
6.1.7 Filtering and heating.....	59
6.1.8 Acid treatment .....	59
6.1.9 Cyclic voltammetry and fuel cell testing.....	59
6.1.10 Summary of process steps.....	60
6.1.11 Theoretical nanoparticle structure.....	61
6.2 Results and discussion .....	62
6.2.1 Chemical processing .....	62
6.2.2 Fuel cell output .....	62
7 CONCLUSION .....	66
7.1 Overview .....	66
7.2 Future recommendations .....	67
REFERENCES .....	68

## LIST OF TABLES

Table		Page
1.	Reduction methods .....	21
2.	Concentrations of sodium formate used .....	29
3.	Concentrations of sodium borohydride used.....	29
4.	Reducing agent optimization results.....	36
5.	PEMFC performance results .....	38

## LIST OF FIGURES

Figure	Page
1. PEMFC schematic diagram [3] .....	3
2. Bipolar plates in PEMFC [5] .....	4
3. PEMFC cost breakdown [6] .....	6
4. Bipolar plates used in PEMFC [20] .....	12
5. Fuel cell electrical losses [21] .....	14
6. A) Single-walled carbon nanotube, B) multi-walled carbon nanotube [27] .....	15
7. Self-assembled monolayer structure of SDS micelles on MWCNTs [18] .....	18
8. Schematic diagram of core-shell nanoparticle [41] .....	19
9. Experimental setup .....	22
10. Microspray electrode fabrication method .....	24
11. Greenlight test station and single test fuel cell .....	25
12. Flow chart diagram of process steps .....	33
13. Theoretical nanoparticle structure on MWCNT A) after reduction, B) after galvanic displacement .....	34
14. Sodium formate reduced samples .....	36
15. Sodium borohydride samples .....	37
16. PEMFC performance data .....	38
17. TEM images of core-shell catalyst without rinsing.....	40
18. TEM images of core-shell catalyst with rinsing .....	41

Figure	Page
19. Nanoparticle size distribution of both catalysts .....	43
20. TEM images of core-shell catalyst produced without rinsing showing agglomerated particles .....	44
21. TEM images of core-shell catalyst produced with rinsing showing agglomerated particles .....	45
22. Platinum and copper particles in catalyst produced without rinsing (copper are dark, platinum are light) .....	46
23. Platinum and copper particles in catalyst produced with rinsing (copper are dark, platinum are light) .....	47
24. Flow chart diagram of process steps .....	52
25. Theoretical nanoparticle structure on MWCNT A) after reduction, B) after heat treatment, C) after galvanic displacement .....	53
26. A) sample after copper reduction, B) copper sulfate in filter water .	54
27. Filter water after galvanic displacement for A) ethanol process, B) toluene process .....	55
28. Fuel cell output .....	56
29. Flow chart diagram of process steps .....	60
30. Theoretical nanoparticle structure A) after reduction, B) after galvanic displacement, C) after heat treatment .....	61
31. SDS samples after reduction and galvanic displacement .....	62
32. SDS catalyst fuel cell voltage characteristics .....	64

## Chapter 1

### INTRODUCTION

#### 1.1 Background

With a recent shift to a more environmentally conscious society, low-carbon and non-carbon producing energy production methods are being investigated and applied all over the world. Government labs and universities all over the world have been researching methods to reduce the cost of alternative energy technologies while increasing the power producing capacity of each technology. These alternative energy technologies include but are not limited to: solar photovoltaics, concentrating solar power, wind energy, tidal energy, geothermal energy, hydropower, biofuels, and fuel cells.

A fuel cell is an electrochemical energy conversion device which produces electrical energy from the chemical energy formed when hydrogen and oxygen interact within a conductive medium. Unlike a battery, a fuel cell does not require recharging and instead requires fuel like an internal combustion engine. Theoretically, a fuel cell will continue to produce energy as long as the external fuels containing hydrogen and oxygen are delivered. This rapid, on-demand power producing characteristic of the fuel cell has made it an attractive energy producing device for stationary and automotive applications.

The five most commonly used types of fuel cells are proton exchange membrane fuel cells (PEMFCs), alkaline fuel cells (AFCs), direct methanol fuel cells (DMFCs), molten carbonate fuel cells (MCFCs), and solid oxide fuel cells (SOFCs). PEMFCs, AFCs, and DMFCs are commonly used for low-temperature

and low-power applications of 25°C - 200°C and 10W - 10kW, respectively. SOFCs and MCFCs are commonly used for high-temperature and high-power applications of 500°C - 1200°C and 10kW - 10MW, respectively. Among the fuel cell types, PEMFCs have received the most research for small scale stationary applications and automotive applications [1]. This interest is due to the PEMFC's unique characteristics of relatively low operating temperature (25°C - 80°C), relatively high power density (1 - 3 W.cm<sup>-2</sup>), and nearly instantaneous start and stop capability.

The PEMFC is composed of three major components: catalyst coated membrane (CCM), gas diffusion layer (GDL), and gas channel conductor plate, as seen in Figure 1 on the following page. The CCM is composed of a proton exchange membrane, electrocatalyst material, and catalyst support material. The proton exchange membrane allows hydrogen cations to pass through its semi-porous material while electrons are blocked. It is ionically conductive and is composed of sulfonated Teflon ® material which is conductive to cations, but not to anions or electrons. The electrocatalyst material increases the kinetics of the chemical reactions and is composed of nano-sized metal, typically platinum. The catalyst support material allows nano-sized metals to be homogeneously deposited onto the membrane and protects the catalyst metal from oxidation and agglomeration [2]. The catalyst support material is usually composed of carbon material which is synthesized with nanocatalyst metal then coated directly on each side of the membrane, forming two electrodes (anode and cathode) and one electrolyte.



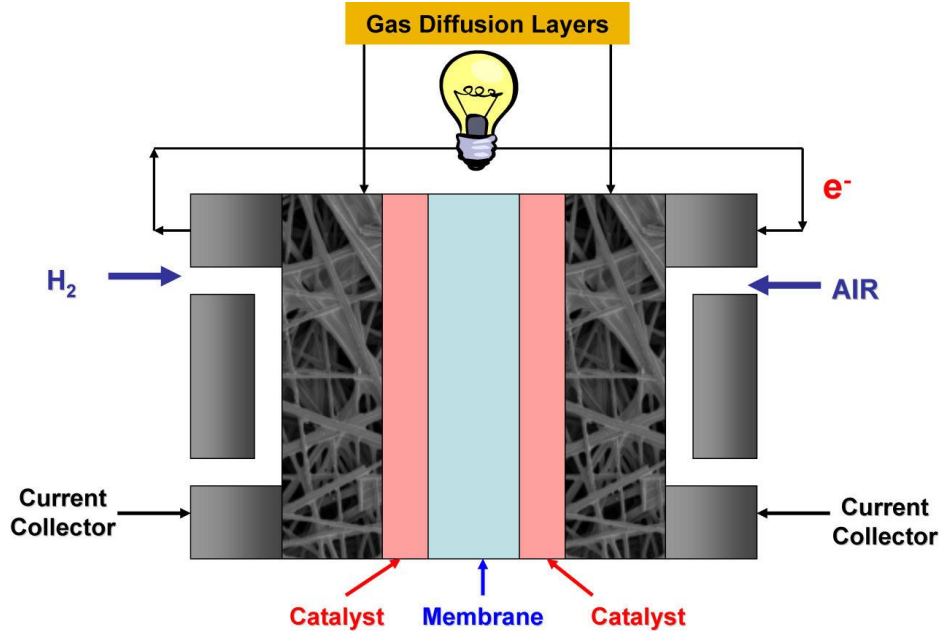


Figure 1 PEMFC schematic diagram [3]

The GDL is composed of porous carbon paper or cloth which is placed on both sides of the CCM to form a conductive layer between the electrode and the gas channels. The GDL also helps distribute the gas across the entire active area by dispersing the gas molecules from the flow fields across its entire area then allowing the gas to pass through to the electrode. The GDL together with the CCM make up the membrane electrode assembly (MEA) which is more often referred to than the individual components themselves.

The gas channel conductor plate is an electrically conductive plate with gas channels etched onto the surface which allows gas to flow across the active area of the electrode. In a single PEMFC, the conductive plate will only be exposed to one gas and will serve as one electrode. In multi-membrane PEMFCs, known as PEMFC stacks, very thin conductive metal plates, known as bipolar

plates are used. Bipolar plates have gas channels on both sides of the surface, allowing both hydrogen and oxygen gases to flow along their surface. This allows one plate to be used as both anode and cathode electrodes [4]. Figure 2 shows a schematic diagram of bipolar plates in a PEMFC.

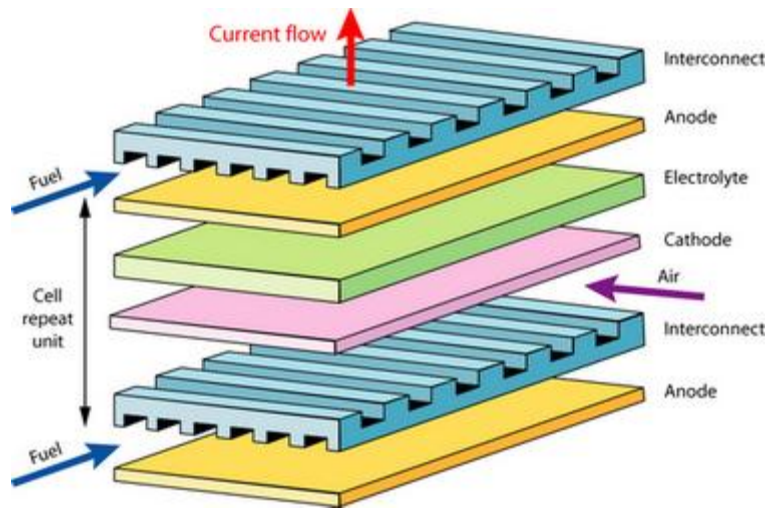


Figure 2 Bipolar plates in PEMFC [5]

The chemical reactions in a PEMFC occur at the anode (negative electrode) and the cathode (positive electrode). The proton exchange membrane only allows the hydrogen proton to pass through while the electron is blocked. This causes the hydrogen atom to be oxidized, losing an electron while the  $H^+$  ion passes through the membrane to the cathode. This reaction in which hydrogen loses an electron is known as a hydrogen oxidation reaction (HOR). The free electron formed by this reaction is in an active state containing electrical energy and forced through an external circuit which allows it to be used to power a load. The electron then loses its energy and is passed to the cathode. At the cathode, oxygen is reduced in an oxygen reduction reaction (ORR), forming  $O_2^-$ . The  $H^+$  cations, electrons, and  $O_2^-$  ions recombine to form water ( $H_2O$ ) and heat.

The chemical reactions in a fuel cell are thus:

- 1) Anode:  $2\text{H}_2 (\text{g}) \rightarrow 4\text{H}^+ (\text{aq}) + 4\text{e}^-$
- 2) Cathode:  $2\text{O}_2 (\text{g}) + 4\text{H}^+ (\text{aq}) + 4\text{e}^- \rightarrow 2\text{H}_2\text{O} (\text{l})$
- 3) Overall:  $2\text{H}_2 + \text{O}_2 \rightarrow 2\text{H}_2\text{O} + \text{electricity} + \text{heat}$

## 1.2 Statement of problem

In order for PEMFC technology to reach wide-scale commercialization it must overcome three critical barriers: cost, performance, and reliability. In order to compete with other stationary power generation systems and with the internal combustion engine (ICE) currently used in automotive vehicles, the cost of the PEMFC should be dramatically reduced. According to the US Department of Energy (DOE), fuel cell system costs have dramatically reduced over the past decade, yet still need to be sharply reduced to be competitive [6]. In 2008, the TIAX, LLC fuel cell team provided the cost analysis of PEMFC manufacturing for automotive applications, shown in Figure 3. Over half of the cost (54 percent) is composed of the platinum (Pt) based electrode [4]. Therefore, most of the cost reduction needs to be based on the electrode material, namely the expensive Pt catalyst. Many different catalyst materials have been studied for use in PEMFCs, however it has been shown that none have matched the electrical output capable of Pt based PEMFCs [7, 8, 9].

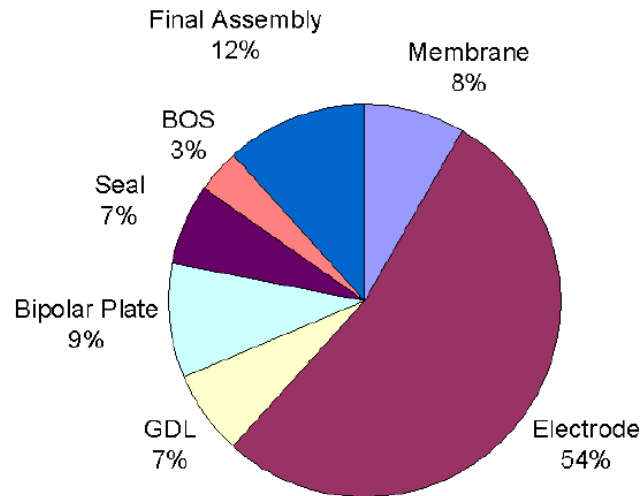


Figure 3 PEMFC cost breakdown [6]

Although cost is one the critical technical challenges of PEMFCs, performance and reliability need to be equally considered. Platinum allows for high electrical output due to its ability to act as an effective catalyst in a PEMFC. This is due to its ability to decrease the activation energy needed to complete the ORR at the cathode by increasing the kinetics of the ORR [10]. The exchange current density, which directly affects catalytic activity, is much greater for platinum than other metals [11]. Platinum is also greater on the electromotive scale than other metals [12]. It is also a very stable material that is not easily oxidized and it can be subjected to electrical currents for extended periods of time [13]. These characteristics allow Pt catalyst to provide relatively higher electrical power and greater durability than less expensive materials. New lower cost catalyst materials developed for PEMFC technology must not only be less expensive than Pt, but must also possess relatively similar or improved performance and durability characteristics in the PEMFC.

The focus of this thesis is to develop a Pt based catalyst material with reduced cost. In order to obtain this goal, platinum-on-copper (Pt@Cu) core-shell nanocatalyst was developed. This material consists of a copper-platinum alloy core which is surrounded by platinum metal. Since only the shell interacts with gases in the fuel cell, the material's behavior in a fuel cell is similar to that of a platinum nanoparticle. This nanoparticle catalyst is synthesized with multi-walled carbon nanotubes (MWCNT) support material to achieve optimum catalyst activity resulting in high power output.

### 1.3 Scope of work

The work presented in this thesis is designed to achieve the following objectives:

- 1) Development of Pt@Cu core-shell nanocatalyst on MWNCT support using three synthesis methods
  - a) Investigation of direct deposition synthesis method
  - b) Investigation of two-phase surfactant synthesis method
  - c) Investigation of single-phase surfactant synthesis method
- 2) Evaluation of Pt@Cu nanocatalyst on MWNCT support
  - a) Visual evaluation of chemical reactions
  - b) Evaluation of PEMFC performance using PEMFC test station
  - c) Characterization of Pt@Cu / MWCNTs by transmission electron microscopy (TEM)

### 1.4 Organization of thesis

This Thesis is composed of seven chapters:

- 1) Chapter 1 gives an introduction to the thesis including background information and the scope of the work.
- 2) Chapter 2 gives a detailed literature review of PEMFC technology, the challenges facing the technology, and related work conducted by others which has been invaluable to the current work in this thesis.
- 3) Chapter 3 discusses the experimental methodology including materials, processes, and procedures used in development and characterization of the nanocatalyst material
- 4) Chapter 4 discusses the methodology and experimental details of the direct deposition synthesis method as well as the results of experimentation.
- 5) Chapter 5 discusses the methodology and experimental details of the two-phase surfactant synthesis method as well as the results of experimentation.
- 6) Chapter 6 discusses the methodology and experimental details of the single-phase surfactant synthesis method as well as the results of experimentation.
- 7) Chapter 7 provides the conclusions drawn from experimentation as well as future recommendations.

## Chapter 2

### LITERATURE REVIEW

#### 2.1 Fuel cell history

The concept of a fuel cell was first demonstrated by Sir William Grove in 1839. Sir William Grove used two Pt electrodes in glass bottles, one containing hydrogen gas and the other containing oxygen, submerged in sulfuric acid to produce electricity [14]. The first PEMFC was developed by Thomas Grubb and Leonard Niedrach at General Electric Company ®. Due to the high cost of the PEMFC, it was only used for limited applications, primarily space applications. During the 1980s and 1990s, PEMFCs were further developed due to an increase in research funding. The cost of a fuel cell system was significantly reduced and PEMFCs were demonstrated for more applications, including automotive transportation. Research is still being conducted to further reduce the cost of the system and enable fuel cell systems for automotive applications to be comparable with the internal combustion engine. Most of the research and development conducted on fuel cell systems involves increasing the conductivity of the GDL, reducing the thickness of the membrane, and reducing the amount of Pt used in the electrodes.

#### 2.2 Technical challenges for fuel cells

In order for fuel cell technology to become commercially viable, three main technical challenges must be controlled: cost, durability, and performance [6]. In order to become viable for automotive applications, PEMFC technology must compete with the internal combustion engine (ICE) currently used in

vehicles. The US Department of Energy (DOE) has set standards for the cost, weight, and power density of a PEMFC system. These standards are set to ensure PEMFCs used for automotive applications will be as reliable and durable as the modern ICE.

### 2.2.1 Cost

The MEA makes up a large portion of the PEMFC cost, which has steered many researchers to develop methods to maximize the utilization of the MEA materials. These methods include maximizing the catalyst utilization by using smaller catalyst materials and using highly conductive, high surface area catalyst support materials [15].

The effectiveness of the catalyst is directly dependant on its electrochemically active surface area (ESA). Electrochemically active surface area is the surface area of the material available for electrochemical interaction [16]. Increasing the ESA of the catalyst material allows more of the active material to interact with gas molecules within the fuel cell. Greater ESA will result in greater power output since more catalyst material is exposed to the gas molecules. In order to increase the ESA of the catalyst material, nanoparticles with diameters of two to ten nanometers, are formed and deposited on catalyst support material.

### 2.2.2 Durability

The DOE has set durability targets on PEMFCs for automotive and stationary applications. PEMFCs for automotive applications must operate for at least 5,500 operating hours while PEMFCs for stationary applications must



operate for at least 50,000 hours [17]. In order to increase the durability of the PEMFC, new catalyst support materials and new membrane materials are being developed. However, the degradation characteristics of the individual components in the PEMFC are not well known [17]. In addition, durability testing requires many hours of tests, even during accelerated testing [17]. In addition to degradation of the components of the PEMFC, long-term use also causes agglomeration of the catalyst material, decreasing the ESA of the electrode [18].

### 2.2.3 Performance

The DOE has also set targets for the power output per kg of weight of a PEMFC stack. The DOE 2015 target for automotive PEMFCs is 650 W/kg [19]. In order to reach this goal, all of the PEMFC components need to be as light as possible and must be as electrically conductive as possible. To achieve high power output with light weight, bipolar plates are used as gas transfer channels and conductive plates. The bipolar plate acts as both the anode and cathode electrodes and allows only hydrogen to pass on one side while only allowing oxygen to pass on the other side. Bipolar plates, shown in Figure 4, eliminate the need for bulky graphite conductive plates which weigh much more than bipolar plates and can only be used for one electrode.

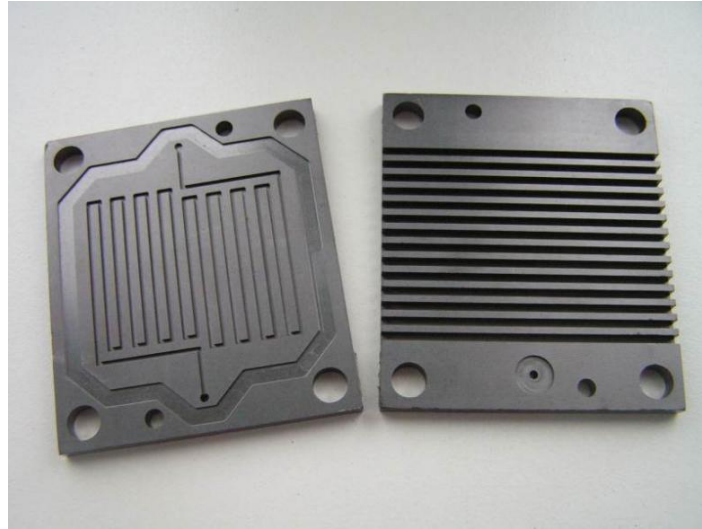


Figure 4 Bipolar plate used in PEMFC [20]

Another method used to increase the PEMFC power output is to decrease the thickness of the membrane. By reducing the thickness of the membrane, its resistance to allow hydrogen protons to pass through is reduced. The membrane thus becomes more conductive. Reducing the thickness of the membrane also increases its conductivity from the electrode to the collector plate, aiding in the oxygen reduction reaction.

### 2.3 Fuel cell electrical losses

There are three main types of losses that occur in a PEMFC: activation losses, ohmic losses, and mass transport and concentration losses. Activation losses are caused by the delay of the reactions taking place at the electrochemical sites on the electrode. In order to decrease activation losses, the kinetics of the chemical reactions must be increased. This can be done by increasing the cell temperature, increasing the gas flow, using more effective catalysts, and by increasing the pressure of the gas.

Ohmic losses are caused by internal resistance in electrode conductivity, membrane, GDL, and collector plate. In order to decrease the ohmic losses in a PEMFC, the conductivity of the materials used must be as high as possible. Furthermore, the ohmic losses can also be reduced by increasing the cell temperature and using more effective catalyst materials which have less resistivity.

Mass transport losses are caused by the slow kinetics of removing used oxygen and water out of the cell. When water is produced at the cathode and builds up without being removed, it forms resistance between the gas and the electrode, reducing the kinetics of the ORR. This is known as flooding of the cell. When the cell becomes flooded, the oxidant gas cannot flow freely out of the cell and causes resistance to entering gas. Flooding often occurs when the fuel cell operates at lower voltages and higher current is drawn, producing more water at the cathode.

Concentration losses are caused by a reduction in the concentration of oxygen in the oxidant gas. Rather than using pure oxygen, air is usually used as the oxidant fuel for a PEMFC. Since air is roughly twenty percent oxygen, the concentration of oxygen molecules at the cathode will not be as great as when pure oxygen gas is used. As a result, the power output of the cell is significantly reduced when air is used as the oxidant. In order to decrease the concentration losses, the oxidant gas is pressurized to increase the amount of oxygen available to react.

Each of these losses affect the overall power output of the cell, but occur during different operating conditions. Activation losses occur immediately after current is drawn from the cell. Ohmic losses occur during normal operation of the cell (0.8V – 0.5V). Mass transport and concentration losses occur at low operating voltages. The schematic of the operating range at which these losses occur is shown in Figure 5.

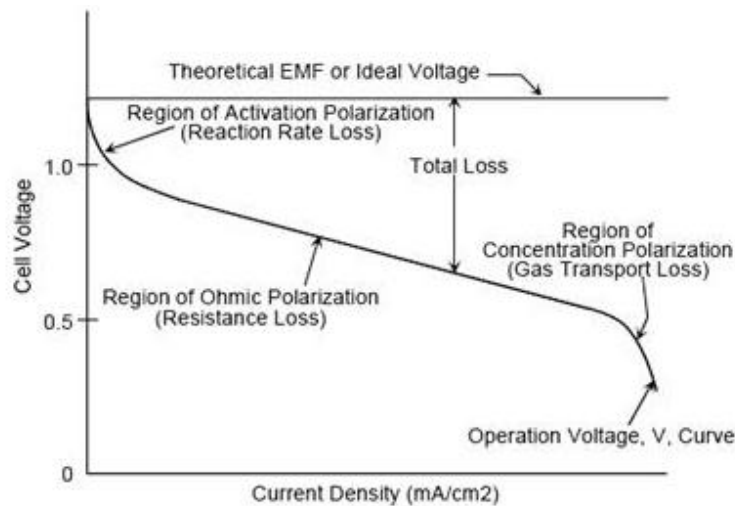


Figure 5 Fuel cell electrical losses [21]

## 2.4 Electrocatalyst support materials

Many catalyst support materials have been investigated for use in PEMFCs. These include but are not limited to: high surface area carbon [22], boron-doped carbon [23], carbon nanofibers [24], and carbon nanotubes (CNTs) [15, 25]. Carbon nanotubes have characteristics such as high conductivity, high mechanical strength, and resistivity to oxidation which make them a highly researched material in recent publications [26].

Carbon nanotubes are a form of graphitic carbon which grows into rolled sheets in high temperature conditions. As seen in Figure 6, carbon nanotubes can be made of a single rolled sheet, known as single-walled carbon nanotubes (SWCNTs) or of many layers of rolled sheets, known as multi-walled carbon nanotubes (MWCNTs). Multi-walled carbon nanotubes are grown using different methods, *i.e.* arc discharge, laser ablation, and chemical vapor deposition (CVD). Chemical vapor deposition has been shown to grow kilograms of MWCNTs commercially and is currently the most cost effective method of MWCNT growth.

In fuel cell applications, MWCNTs serve as effective catalyst support due to their high surface area provided by their size and shape. As seen in Figure 6, MWCNTs have cylindrical shape with high surface area available for depositing nanometals [27].

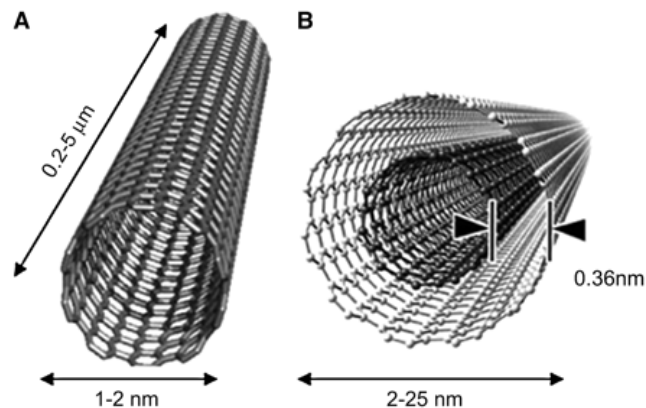


Figure 6 A) Single-walled carbon nanotube, B) multi-walled carbon nanotube [27]

## 2.5 Functionalization of multi-walled carbon nanotubes

Multi-walled carbon nanotubes have inert surfaces that are not reactive and allow them to clump together in forests due to Van der Waals force. They are

hydrophobic and do not disperse in water. In order to create anchoring sites on the carbon nanotube surface and in order to improve the wetting characteristics of the nanotubes, carbon nanotubes are functionalized to create functional groups such as hydroxyl (-OH) and carboxyl (-COOH) groups on the nanotube surface [28]. Functionalization of multi-walled carbon nanotubes can be achieved using polymer based surfactant materials, chemical treatment with acid, electrochemical modification, and photochemical treatment [28, 29, 30].

Previous research conducted at the Arizona State University Fuel Cell Laboratory has shown citric acid treatment to be an effective functionalization method for MWCNTs [15,31]. The use of strong acids can cause defects in the nanotube structure, shortening the tubes and causing them to curl [30]. The use of citric acid allows for the formation of hydroxyl and carboxyl functional groups on the surface of the carbon nanotube without causing defects [15, 28].

## 2.6 Surfactant materials

The use of surfactant materials has been shown to control particle size and distribution of nanoparticles deposited on carbon support [15,18,31]. Many surfactant materials have been used for nanoparticle synthesis such as polymers, thiols, and micelles [18, 29, 31]. In this study, dodecanethiol (DDT), an alkanethiol frequently used in the formation of self-assembled monolayers for use in nanoparticle synthesis, is used. Alkanethiols have unique properties which allow them to spontaneously form self-assembled monolayers on surfaces [32]. Dodecanethiol has been used to control particle size during nanoparticle synthesis [33, 34]. Previous research conducted with Lin *et. al.* investigated the use of

dodecanethiol to homogenously disperse platinum nanoparticles on the surface of MWCNTs with positive results [31].

Sodium dodecyl sulfate (SDS), a water-soluble micelle surfactant is also used in this study. Sodium dodecyl sulfate has been shown to homogenously disperse carbon nanotubes in water at concentrations above its critical micelle concentration of 8 mM [35, 36]. Sodium dodecyl sulfate has also been used to control particle size in nanoparticle synthesis [37]. In previous research conducted with Lin *et. al.*, SDS was shown as an effective surfactant used to disperse carbon nanotubes in water and also to control platinum particle size during nanoparticle synthesis [18]. Figure 7 shows the self-assembled monolayer structure of SDS micelles on the surface of carbon nanotubes. The hydrophilic tail of the SDS micelle attaches to the inert surface of the MWCNT. The negatively charged hydrophobic sulfate head of the micelle repels other micelle capped MWCNTs, overcoming Van der Waals force and allowing dispersion of MWCNTs in water [18].

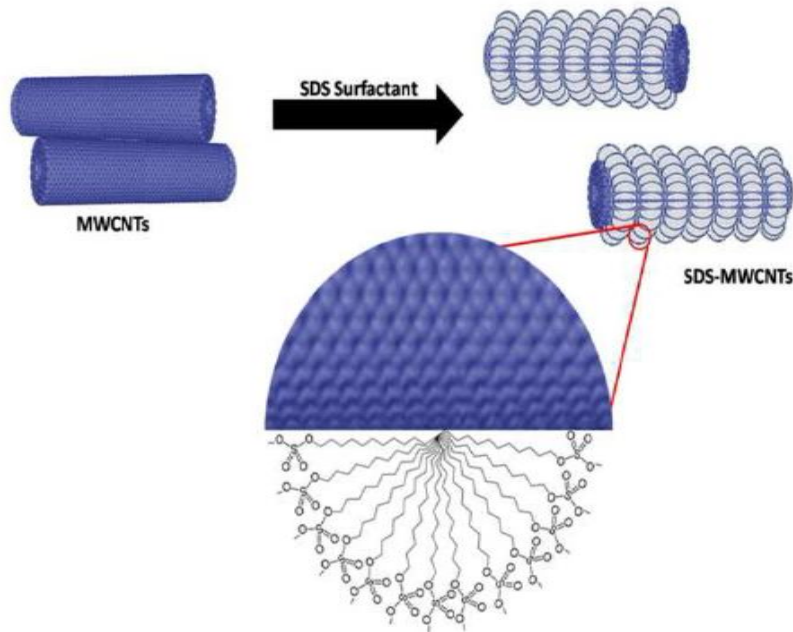


Figure 7 Self-assembled monolayer structure of SDS micelles on MWCNTs [18]

## 2.7 Core-shell nanoparticles

Core-shell nanoparticles are nanoparticles made of two different metals in which one metal completely surrounds another metal creating a core and shell structure [38-40]. The inside material, known as the core, is completely covered with the shell metal, so it is not exposed for chemical reactions [39]. This core-shell structure allows nanoparticles to obtain the characteristics of noble metal nanoparticles while using less of the expensive noble metal. A schematic diagram of a core-shell nanoparticle is shown in Figure 8.



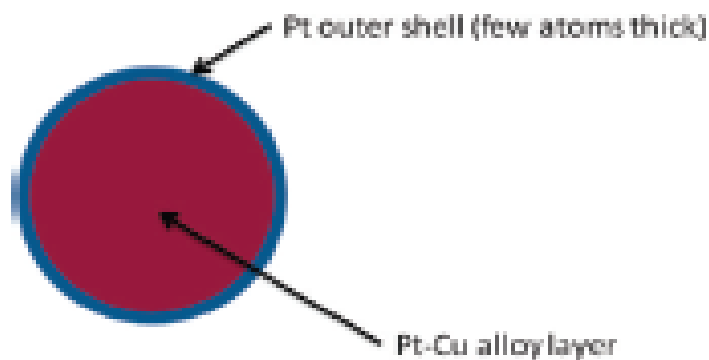
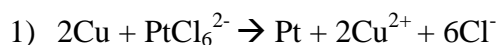


Figure 8 Schematic diagram of core-shell nanoparticle [41]

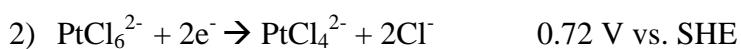
There are different methods used to obtain core-shell nanoparticles. One method uses cyclic voltammetry to de-alloy metal alloys [42]. Other methods use a galvanic displacement chemical reaction in which ions of high electrical potential (electromobility) oxidize metal atoms of lower electrical potential [39-41].

In this study, a unique core-shell nanoparticle synthesis technique developed by A. Sarkar and A. Manthiram of the University of Texas at Austin is adapted to produce platinum-on-copper (Pt@Cu) core-shell nanoparticles with platinum shells and platinum-copper alloy cores [41]. A galvanic displacement reaction spontaneously occurs between copper nanoparticles and  $\text{Pt}^{4+}$  ions in chloroplatinic acid ( $\text{H}_2\text{PtCl}_6 \cdot 6\text{H}_2\text{O}$ ). The reaction [39]:



can occur spontaneously due to the redox potential of the following reactions

which correspond to equilibrium and the corresponding Nernst equations [39]:



In this study the synthesis method developed by A. Sarkar and A. Manthiram was modified to synthesize Pt@Cu nanoparticles on MWCNTs support. To my knowledge, no study has been published for work on Pt@Cu core-shell nanoparticles on MWCNTs support.

## Chapter 3

### METHODOLOGY

#### 3.1 Materials used

In the current study, multi-walled carbon nanotubes (OD 20-30 nm, > 98% purity) were obtained from Cheaptubes Co., copper (II) sulfate pentahydrate ( $\text{CuSO}_4 \cdot 5\text{H}_2\text{O}$ ) and hexachloroplatinic acid ( $\text{H}_2\text{PtCl}_6 \cdot 6\text{H}_2\text{O}$ ) were purchased from Sigma Aldrich. Sodium borohydride ( $\text{NaBH}_4$ ) and sodium dodecyl sulfate ( $\text{C}_{12}\text{H}_{25}\text{SO}_4\text{Na}$ ) were purchased from Fisher Scientific.

#### 3.2 Experimental methods

Three synthesis methods were investigated in order to produce Pt@Cu core-shell nanocatalyst material. As outlined in Table 1, the first method did not use a surfactant material. The second method used the organic surfactant, dodecanethiol, to anchor copper nanoparticles to the surface of multi-walled carbon nanotubes (MWCNTs) before galvanic displacement with platinum ions. The third method used the aqueous surfactant, sodium dodecyl sulfate.

Table 1 Reduction methods

<b>Method</b>	<b>Surfactant used</b>
Direct deposition	none
Two-phase surfactant	Dodecanethiol
Single-phase surfactant	Sodium dodecyl sulfate

### 3.3 Experimental setup

Due to the reduction and oxidation characteristics of copper, byproducts such as copper (I) oxide, copper (II) oxide, and copper hydride can be formed while reducing  $\text{Cu}^{2+}$  ions to copper nanoparticles. In order to prevent oxidation of the copper nanoparticles, reduction must be carried out in an inert environment. During all reactions, the copper sulfate solution was purged with inert gas. In addition, all Deionized (DI) water used was boiled and bubbled with inert gas to remove any excess air content in the water. In order to control the drop-wise addition of salt solutions, a syringe pump (New Era NE-1000) was used. The experimental set-up is shown in Figure 9.

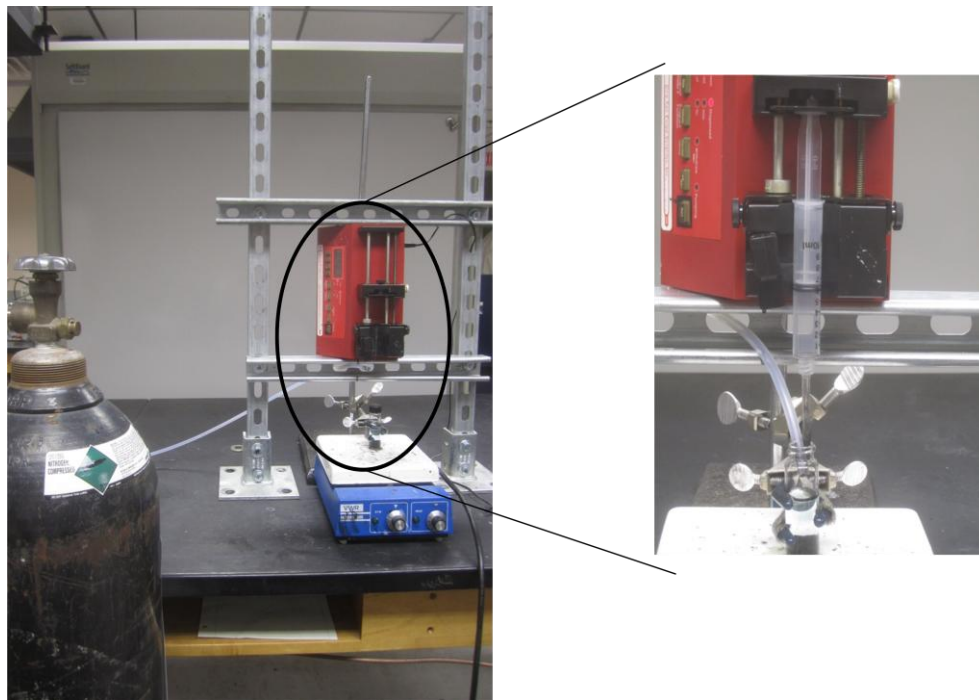


Figure 9 Experimental setup

### 3.4 pH control of copper sulfate solution

Based on literature review, it was determined that the optimum pH for copper sulfate reduction was 3 [41]. Two different solutions were used to obtain a copper sulfate solution with pH 3. The first solution was a 0.04 M solution of glacial acetic acid (GAA). This solution was prepared by adding 4 mL DI water to 10 mg GAA then adding the copper sulfate pentahydrate (CSP) salt to this solution. This solution, however, was found to be difficult to control due to the liquid nature and concentration of GAA. As a result, a second solution with pH 3 containing citric acid (CA) salt in DI water was used. This solution was obtained by adding 100 mL DI water to 45 mg CA salt. The solution was then ultrasonicated for 15 minutes then bubbled with nitrogen for 15 minutes. The CSP salt was added to 10 mL of this solution. The pH of the solution was verified using a pH meter.

### 3.5 Fuel cell fabrication

For catalyst samples, commercial catalyst ink was prepared by adding isopropanol (20 mL for 1 g of electrocatalyst) and 5% wt. Nafion® (Ion Power Inc., New Castle, DE, USA) dispersion agent (10 mL for 1 g electrocatalyst) after purging the platinum/carbon (Pt/C) commercial catalyst (TKK, Japan) powder with inert gas. The multi-walled carbon nanotubes synthesized with Pt@Cu nanoparticles (MWCNTs/Pt@Cu) catalyst was prepared identically, with exception of inert gas purging since it was not needed for MWCNTs/Pt@Cu catalyst.

Catalyst layers (anode and cathode) with 5 cm<sup>2</sup> active area were coated onto the surface of a Nafion-212 ® membrane (Ion Power Inc., New Castle, DE, USA) using the micro-spray method shown in Figure 10. The CCM was vacuum dried at 70°C for 15 minutes before assembly in the test cell.

For MWCNTs/Pt@Cu catalyst, commercial catalyst ink was coated onto the anode side the membrane and MWCNTs/Pt@Cu catalyst ink was coated on the cathode side. For commercial catalyst samples, commercial catalyst was sprayed on both anode and cathode sides of the membrane.



Figure 10 Microspray electrode fabrication method

The MEA was assembled by sandwiching the catalyst coated membrane between two gas diffusion layers inside the single test cell (Fuel Cell Technologies Inc, Albuquerque, NM, USA). Two silicone coated fabric gaskets (Product # CF1007, Saint-Gobain Performance Plastics, USA) were used on both

sides of the MEA for gas sealing. A uniform torque of 40 pounds per square inch was used to tighten the single test cell to provide further gas sealing.

### 3.6 Cyclic voltammetry activation and fuel cell testing

All evaluated catalysts were assembled in the single test cell and characterization was conducted using the Greenlight Test Station (G50 Fuel cell system, Hydrogenics, Vancouver, Canada), shown in Figure 11.



Figure 11 Greenlight test station and single test fuel cell

Cyclic voltammetry was carried out for 100 cycles between open circuit voltage (OCV) and 0.2 V using humidified H<sub>2</sub>/O<sub>2</sub> gases at 25°C and 100% humidity with flow rates of H<sub>2</sub> and O<sub>2</sub> fixed at 200 SCCM and 300 SCCM, respectively, in order to de-alloy the core-shell catalyst [41]. This was

accomplished by a LabView® script written and programmed using the Hydrogenics Hyware II ® software (version 1.0.2.86), which accompanies the Hydrogenics ® test system. Cyclic voltammetry was conducted by increasing the cell current by 200 mA until the cell voltage reached 0.2 V followed by then decreasing the current to 0 A to achieve OCV.

After the cyclic voltammetry cycles, the gas temperatures and fuel cell temperature were elevated to 80°C with 100% gas humidity, and ambient pressure. The flow rates of H<sub>2</sub> and O<sub>2</sub> remained fixed at 200 SCCM and 300 SCCM, respectively. During this temperature increase, the cell was held at a constant voltage of 0.3 V. For samples showing high current potential, polarization data was recorded from open circuit voltage (OCV) to 0.3 V. Current vs. voltage as well as current vs. power curves were obtained from the recorded data.



## Chapter 4

### DIRECT DEPOSITION METHOD

#### 4.1 Experimental details

##### 4.1.1 Fabrication methodology

Platinum on copper core-shell nanoparticles were synthesized with multi-walled carbon nanotubes to produce a highly functional core-shell nanocatalyst. Two reducing agents were used to synthesize copper nanoparticles with MWCNTs then chloroplatinic acid was added to produce a galvanic displacement reaction between copper atoms and platinum ions.

##### 4.1.2 Functionalization of carbon nanotubes

In order to improve the wetting characteristics of the multi-walled carbon nanotubes, the nanotubes were functionalized with citric acid to produce hydroxyl (OH) and carboxyl (COOH) functional groups on the nanotube surface. A 0.9 M solution of citric acid was prepared by adding 500 mg citric acid salt in 1.5 mL DI water. The solution was then ultrasonicated for 15 minutes at room temperature. One hundred milligrams of MWCNTs was added to the solution and the solution was magnetically stirred overnight at room temperature. The solution was then filtered and washed repeatedly with warm DI water in a glass frit filter. The MWCNTs were then heated at 350°C in an oven furnace for 30 minutes then allowed to cool to room temperature.

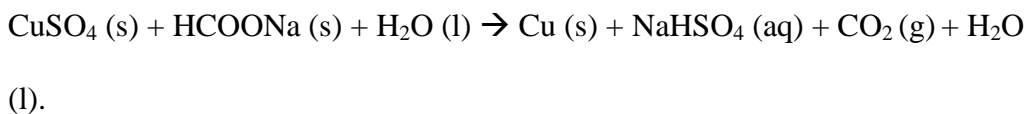
##### 4.1.3 Preparation of copper sulfate solution

A 0.04 M copper sulfate solution was prepared by adding 98 mg copper sulfate pentahydrate to a 10 mL 2mM citric acid solution followed by 15 minutes

ultrasonication. One hundred milligrams CA functionalized MWCNTs were added to the solution and the solution was magnetically stirred for 30 minutes at room temperature under flowing nitrogen before reduction.

#### 4.1.4 Reduction methods

Two reducing agents, sodium formate and sodium borohydride were used to reduce copper ions ( $\text{Cu}^{2+}$ ) to copper nanoparticles in order to determine the optimum reducing agent for copper reduction. The first method used sodium formate to reduce the copper ions in the following reaction:



In this reduction method, various amounts of sodium formate were mixed in a DI water solution and added drop-wise to the copper sulfate solution (4.1.2) at 60°C over a thirty minute period. The solution was then allowed to stir for an additional thirty minutes at 60°C then was left sitting for 30 minutes and allowed to return to room temperature before being evaluated. Evaluation was carried out by observing the color change of the blue copper sulfate solution and whether copper particles were formed on the nanotubes. The concentrations used are shown in Table 2.

Table 2 Concentrations of sodium formate used

Mass of HCOONa (mg)	Volume of DI water (mL)	Molarity (M)
408	6	1
816	6	2
2,040	6	5
4,081	6	10

The other reduction method utilized sodium borohydride as the reducing agent. Reduction of  $\text{Cu}^{2+}$  ions with sodium borohydride was carried out as illustrated by the following formula: [43]

$\text{Cu}^{2+} (\text{aq}) + 2\text{BH}_4^- + 6\text{H}_2\text{O} \rightarrow \text{Cu}(\text{s}) + 7\text{H}_2 + 2\text{B}(\text{OH})_3$ . Since sodium borohydride is a stronger reducing agent than sodium formate, a lower temperature ( $21^\circ\text{C}$ ) and a longer reaction time (two hours) was given for the reaction. Various amounts of sodium borohydride were mixed in a DI water solution then were added to a copper sulfate solution drop-wise over two hours. The solution was then stirred for an additional 30 minutes then was left sitting for 30 minutes before evaluation. The concentrations of sodium borohydride used are shown in Table 3.

Table 3 Concentrations of sodium borohydride used

Mass of $\text{NaBH}_4$ (mg)	Volume of DI water (mL)	Molarity (M)
12	6	0.053
24	6	0.106
36	6	0.16

#### 4.1.5 Evaluation of reaction

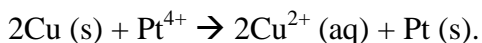
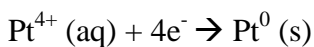
During evaluation, the samples were visually inspected for change in color of the copper sulfate solution. If the solution changed from blue to clear, reduction was complete. If the color became lighter, reduction occurred, but not to completion. If the color remained the same, no reaction had taken place. The samples were also inspected for visible copper particles which would indicate improper particle size. Samples which showed positive results from visual evaluation moved on to the next process steps. Samples which showed poor results from visual evaluation were not processed further.

#### 4.1.6 Rinsing and galvanic displacement

Two processes were used to complete galvanic displacement between copper and platinum. In one process, the sample was left untreated before adding chloroplatinic acid. In the other process, the sample was rinsed with DI water before adding chloroplatinic acid. This was done by first removing the aqueous solvent from the vial with a 20 gauge syringe needle then replacing the extracted solvent with 8 mL of DI water. This was completed under flowing nitrogen to protect the copper nanoparticles from oxidation.

A 10 mM solution of chloroplatinic acid was prepared by adding 12 mg chloroplatinic acid salt to 3 mL DI water followed by 15 minutes ultrasonication. The solution was then drop-wise added to the MWCNTs/ Cu solution over two hours at room temperature under flowing nitrogen. During this time, a galvanic displacement reaction occurred between copper nanoparticles and platinum ions

(Pt<sup>4+</sup>) to replace the outer layer of the copper nanoparticles with platinum metal in the following reaction:



#### 4.1.7 Filtering and washing

After galvanic displacement, the MWCNTs/Pt@Cu catalyst material was filtered and washed repeatedly with warm DI water in a glass frit filter. The catalyst material was then dried overnight at 70°C before electrode fabrication.

#### 4.1.8 Acid treatment

After filtering and washing, the MWCNTs/Pt@Cu catalyst powder was added to a 10 mL 9 M sulfuric acid solution. The mixture was stirred for six hours at room temperature then was filtered and washed repeatedly with warm DI water. The purpose of the acid treatment was to remove excess copper which had not reacted with platinum [41]. The sulfuric acid dissolved the un-reacted copper, removing copper from the particle shell and also removing un-reacted copper nanoparticles.

#### 4.1.9 Cyclic voltammetry activation

Cyclic voltammetry activation and de-alloying was conducted as described in section 3.6 of chapter 3.

#### 4.1.10 Summary of process steps

A flow chart diagram of the process steps used to synthesize Pt@Cu nanoparticles with MWCNTs is shown in Figure 12. The completeness of the

reaction was determined using visual observation based on the color of the aqueous solvent and any byproducts visible in the solvent. Samples which showed an incomplete reaction were not processed further and the observations were noted. Samples which were observed to have complete reaction were further processed using two different processing techniques.

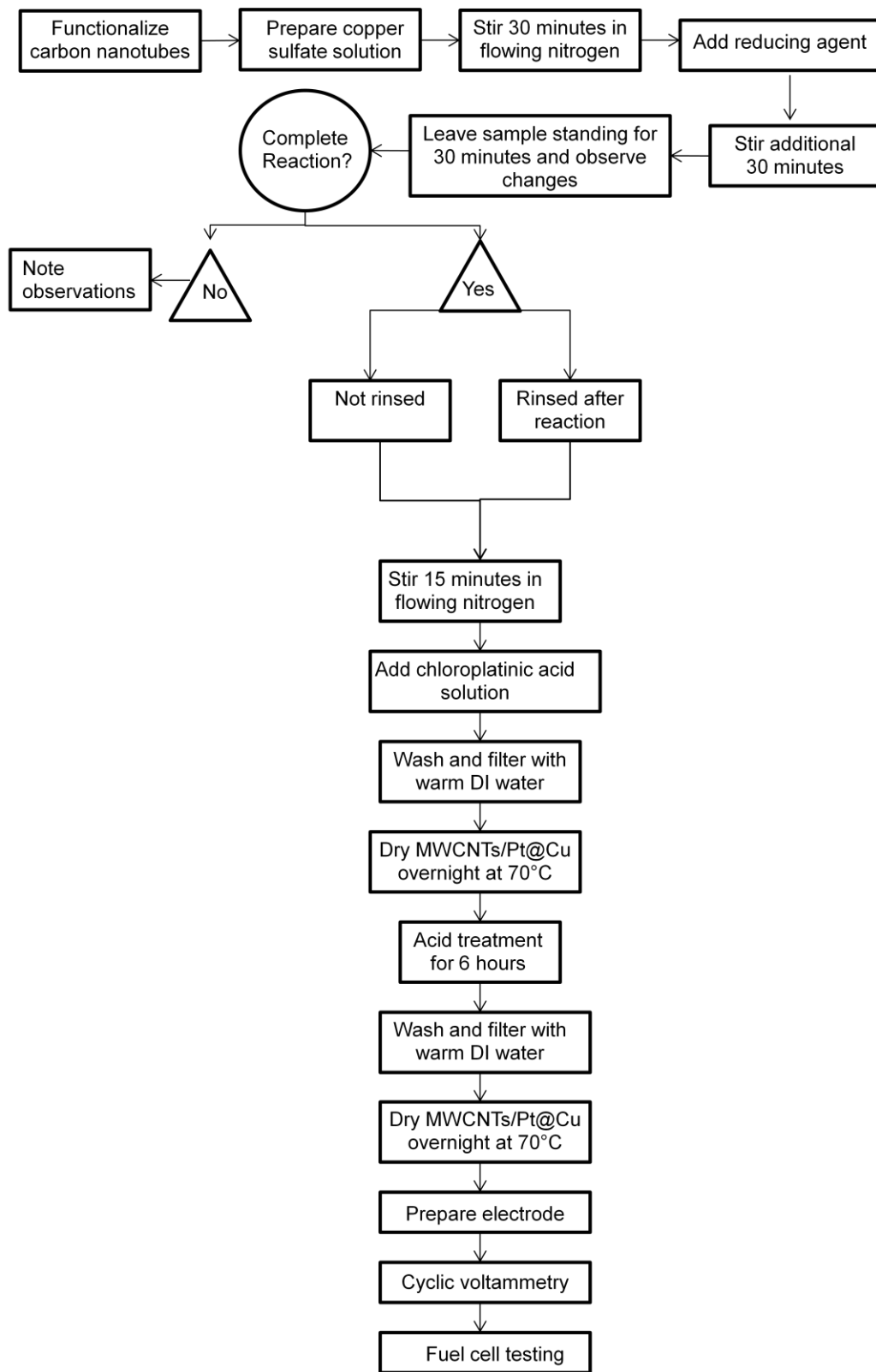


Figure 12 Flow chart diagram of process steps

#### 4.1.11 Theoretical nanoparticle structure

Figure 13 shows theoretical nanoparticle structure on the MWCNT.

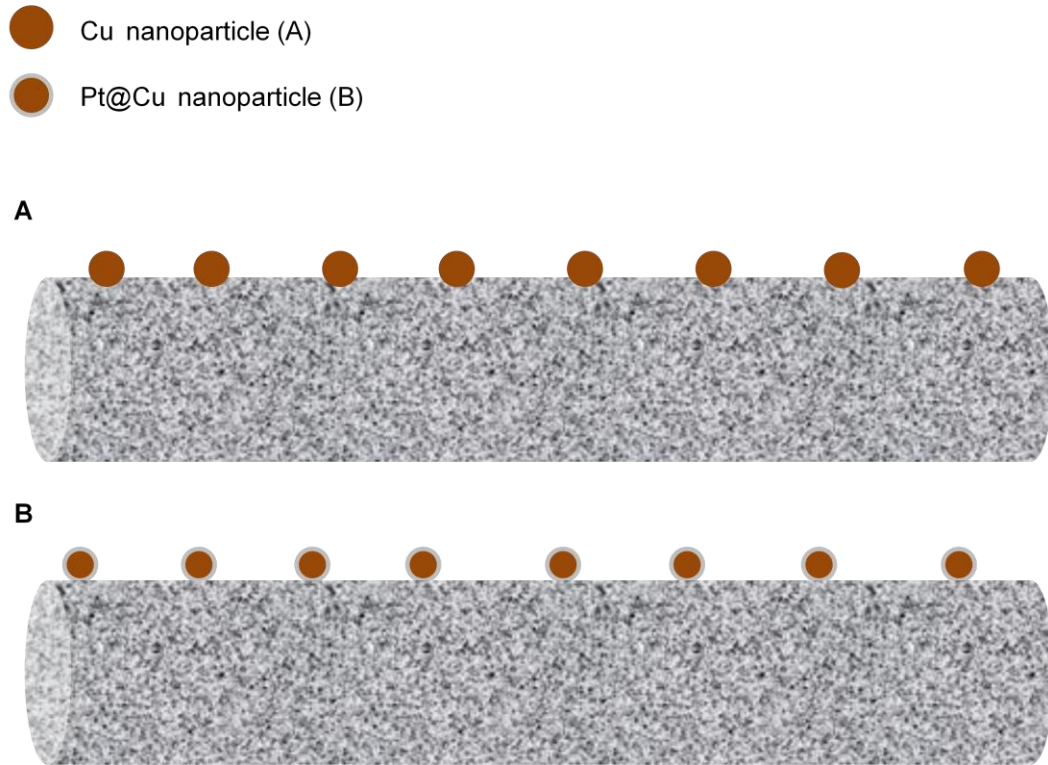


Figure 13 Theoretical nanoparticle structure on MWCNT A) after reduction B) after galvanic displacement

#### 4.1.12 Characterization

The MWCNTs/Pt@Cu catalyst was characterized by visual inspection, fuel cell performance, and transmission electron microscopy (TEM) imaging. Visual inspection was conducted to determine optimum reducing agent and concentration. Samples which were processed further were evaluated by TEM imaging and fuel cell performance.

The MWCNTs/Pt@Cu catalyst was prepared for fuel cell testing as described in sections 3.5 and 3.6 of chapter 3. The platinum loading of both



anode and cathode electrodes (separately) for MWCNTs/Cu samples was  $0.1 \text{ mg Pt.cm}^{-2}$ . Platinum loadings of the anode and cathode electrodes for commercial catalyst samples were  $0.1 \text{ mg.cm}^{-2}$  (anode and cathode, separately) for the low loading sample and  $0.1 \text{ mg.cm}^{-2}$  (anode),  $0.3 \text{ mg.cm}^{-2}$  (cathode) for the high loading sample.

The Pt@Cu core-shell nanoparticle dispersion and particle size of the catalyst sample was characterized by transmission electron microscopy using Phillips CM200-FEG. Core-shell nanocatalyst dispersed in methanol was applied on a lacy carbon grid for TEM characterization.

## 4.2 Results and discussion

### 4.2.1 Chemical reduction

The results of reducing agent optimization are shown in Table 4. Sodium formate was shown to be an insufficient reducing agent to reduce  $\text{Cu}^{2+}$  ions to copper nanoparticles. Figure 14 shows samples with corresponding Molarity of sodium formate. Even at very high Molarity, sodium formate had no affect on the  $\text{Cu}^{2+}$  ions. As a result, sodium formate could not used as a reducing agent to form Pt@Cu core-shell nanocatalyst.

Table 4 Reducing agent optimization results

Sample	Reducing agent	Molarity	Result
1	HCOONa	1	Incomplete reduction
2	HCOONa	2	Incomplete reduction
3	HCOONa	5	Incomplete reduction
4	HCOONa	10	Incomplete reduction
5	NaBH <sub>4</sub>	0.053	Incomplete reduction
6	NaBH <sub>4</sub>	0.106	Formation of large copper particles/ films
7	NaBH <sub>4</sub>	0.16	Formation of copper nanoparticles on MWCNTs

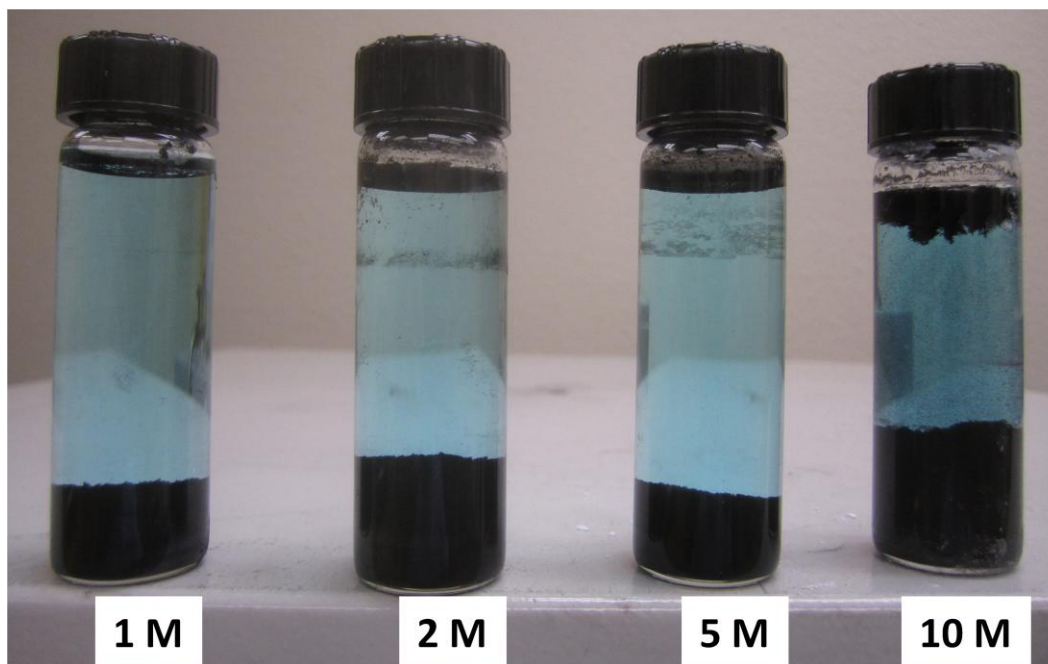


Figure 14 Sodium formate reduced samples

Sodium borohydride, however, was shown to be an effective reducing agent to reduce copper ions to copper metal. Figure 15 shows samples with

corresponding Molarity of sodium borohydride. Although some reaction occurred with the addition of a 0.053 M solution, the reaction was incomplete and copper sulfate remained in the solution. During the addition of a 0.106 M solution, large copper films formed at the surface of the solution. Since the films formed at the top, the copper was forming in the solution and not on the nanotubes. A 0.106 M solution was therefore concluded insufficient for copper reduction. A 0.16 M solution, however, did not form copper at the top of the solution and the solution became clear after addition of the solution. Copper nanoparticles had formed on the surface of the nanotubes and only reaction byproducts remained in the solution.

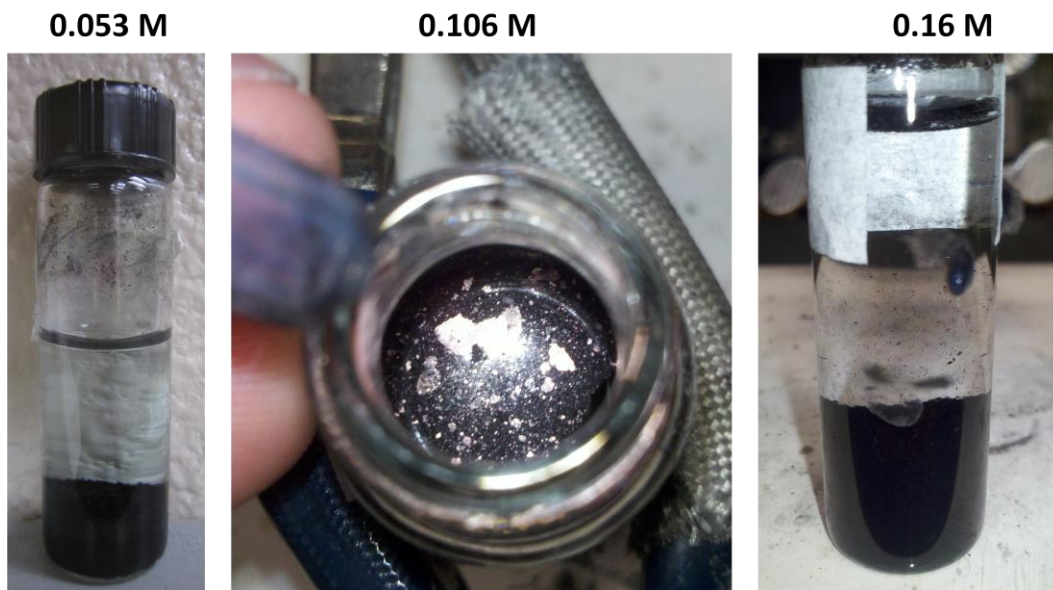


Figure 15 Sodium borohydride reduced samples

#### 4.2.2 Fuel cell test results

Upon first beginning the cyclic voltammetry cycles (first 20 cycles), the OCV of the cell for both methods was relatively low (around 0.7 V) and the

current density was relatively low (around  $100\text{mA}\cdot\text{cm}^{-2}$ ). The OCV and the current density began to increase for both cells as the cycles were conducted then leveled off around 100 cycles. As the temperature of the cell was increased for testing, the current density increased and leveled off as  $80^\circ\text{C}$  was reached. The polarization data obtained is shown in Table 5 and Figure 16.

Table 5 PEMFC performance results

Catalyst	Peak power density ( $\text{mW}\cdot\text{cm}^{-2}$ )
MWCNTs/Pt@Cu without rinsing	273
MWCNTs/Pt@Cu with rinsing	618
Commercial catalyst high loading (0.3 mg cathode loading)	734
Commercial catalyst low loading (0.1 mg cathode loading)	539

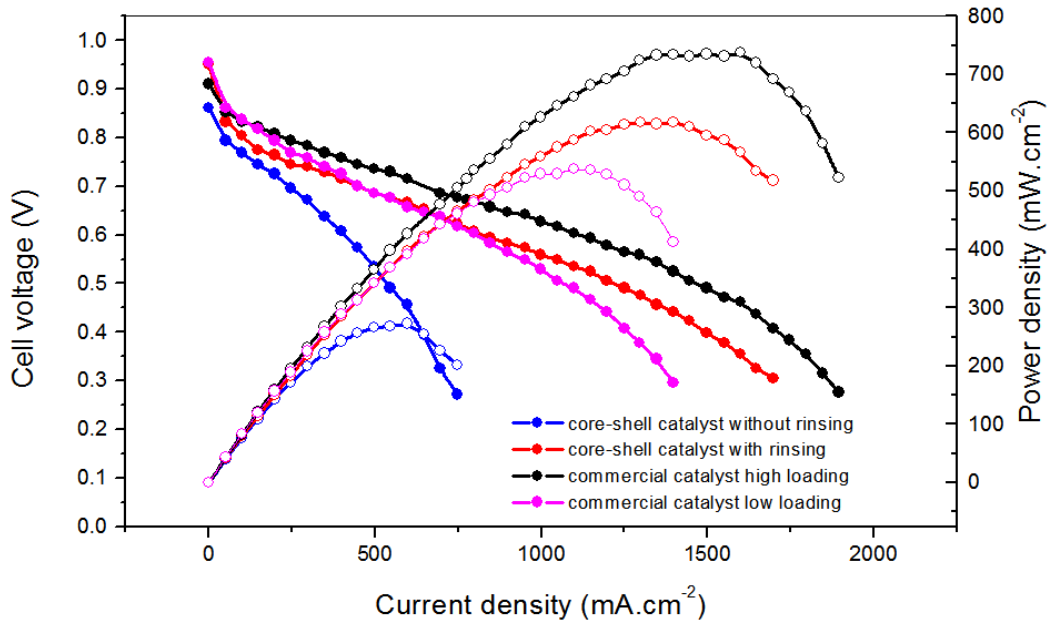


Figure 16 PEMFC performance data

As seen in Table 5, the MWCNTs/Pt@Cu catalyst which was rinsed before the addition of platinum showed the highest current density for a 0.1 mg.cm<sup>-2</sup> Pt loading. The peak power density of core-shell catalyst synthesized using the rinsing process was 618 mW.cm<sup>-2</sup>, 13 percent greater than that of commercial catalyst with similar loading and only 16 percent less commercial catalyst with three times the platinum loading. This high power density shows great potential for MWCNTs/Pt@Cu nanocatalyst due to its high utilization of platinum material.

Catalyst synthesized without rinsing before the addition of platinum, however, showed very low power density, peaking at 238 mW.cm<sup>-2</sup>. The OCV as well as the current and power densities were much lower for catalyst synthesized without the rinsing process.

#### 4.2.3 Microscopic imaging

Transmission electron microscopy revealed that both catalysts produced were composed of core-shell nanocatalyst, but the utilization of platinum varied between the two. As seen in Figures 17 and 18, both catalysts contained Pt@Cu nanoparticles on the MWCNT surface, but the catalyst synthesized using the rinsing process had few platinum nanoparticles on the MWCNT surface while the catalyst synthesized which was not rinsed had many.

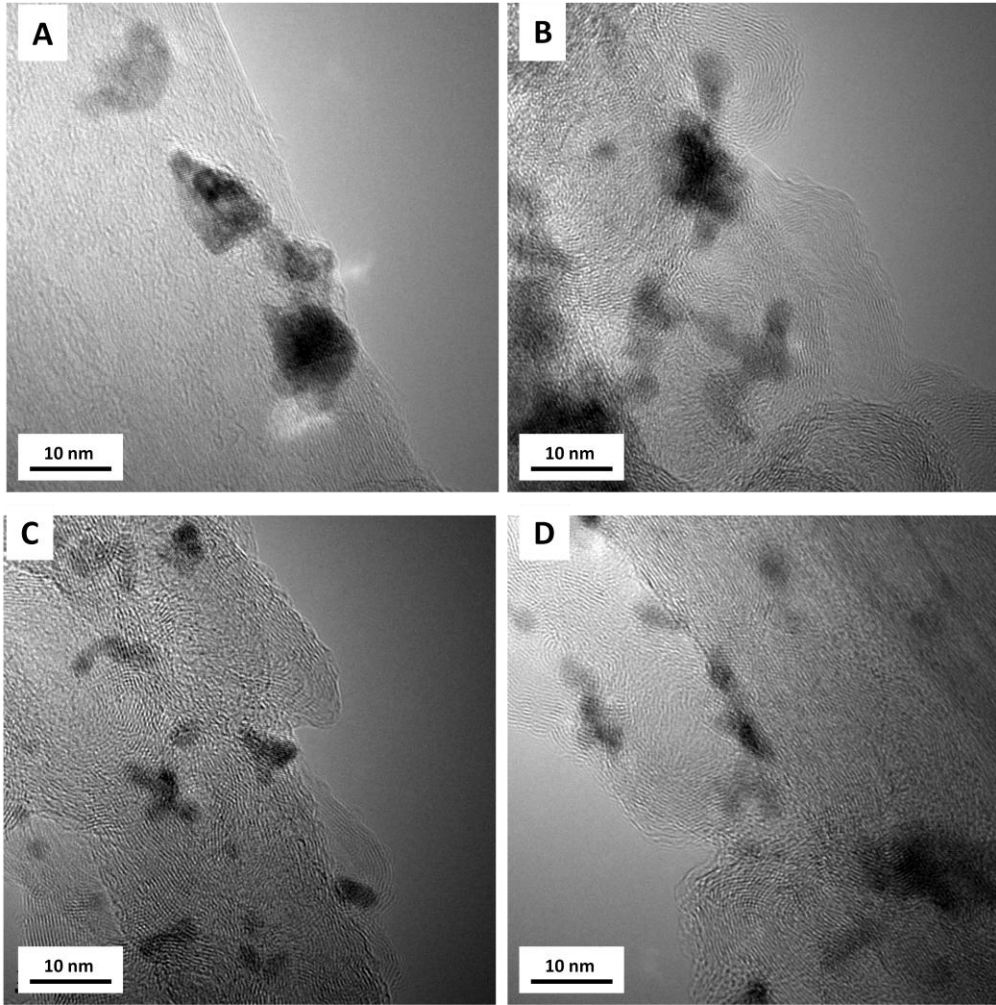


Figure 17 TEM images of core-shell catalyst without rinsing

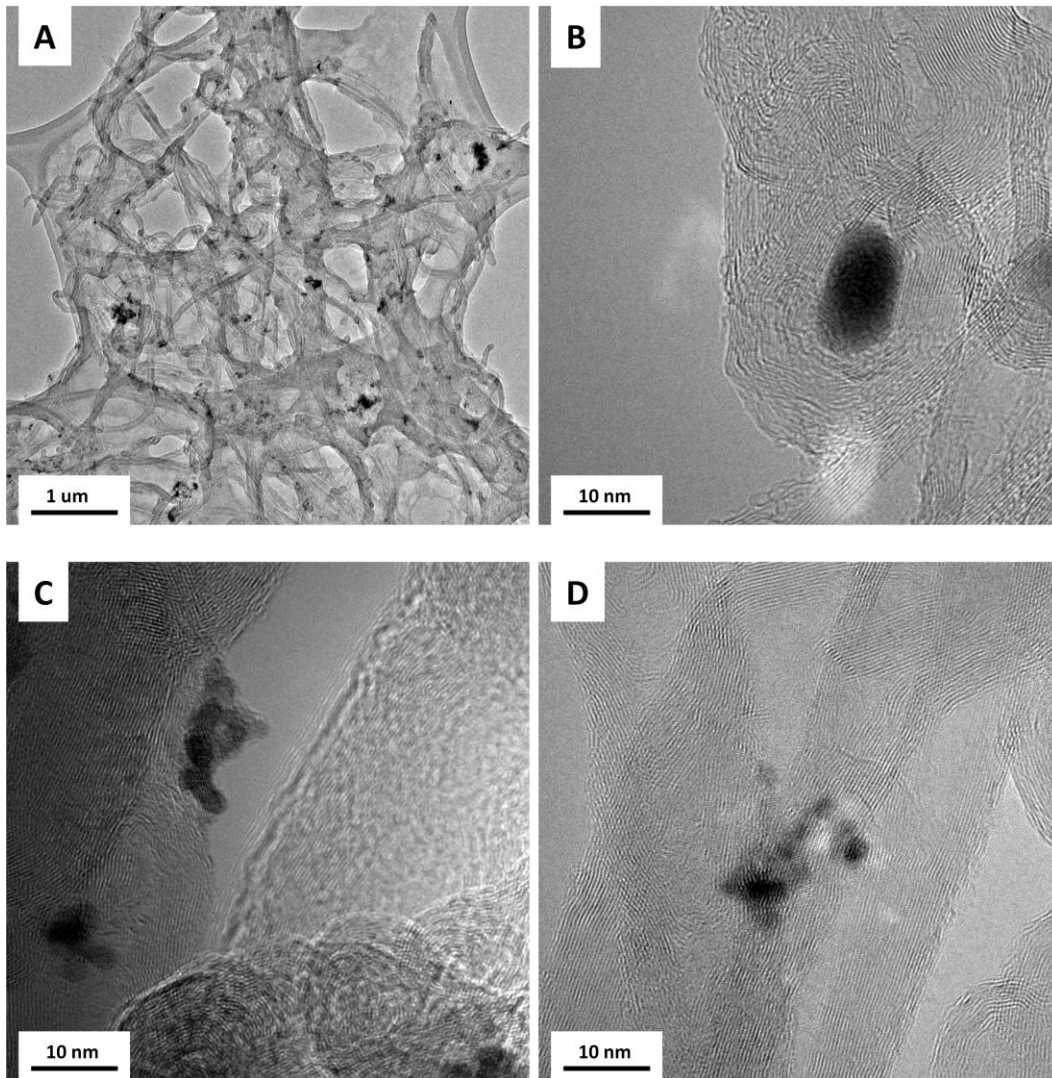


Figure 18 TEM images of core-shell catalyst with rinsing

As is evident by the images, the fabrication methods did not produce perfect core-shell nanoparticles with complete platinum shell and uniform copper core. Instead, the inner portions of the nanoparticles were composed of a platinum-copper alloy with varying ratios of platinum and copper. It is concluded by the images, however, that the nanoparticles produced by the fabrication method indeed have copper-platinum cores and platinum shells. The two-contrast

(dark and light) composition of the nanoparticles is similar to that of other core-shell catalysts and is not a characteristic of pure platinum nanoparticles within close range of the particle size [15, 18, 31, 40- 41,44-46].

It is also evident that the utilization of platinum was more effective for the catalyst which had been rinsed with DI water before adding chloroplatinic acid. When the water was extracted during the rinsing process, any excess reducing agent that had not reacted with copper ions was removed. For catalyst that did not use the rinsing process, the excess reducing agent was left in the solution. As a result, many platinum ions were reduced by the reducing agent and did not react with the copper nanoparticles. In addition, the core-shell nanoparticles were composed mostly of platinum in catalyst produced without the rinsing process and of copper in catalyst produced by using the rinsing process. By having less platinum per particle, the catalyst produced using the rinsing process is able to utilize more platinum surface area than catalyst produced without rinsing.

Both methods produced a mixture of lone core-shell nanoparticles and agglomerated core-shell nanoparticle clusters. The core-shell nanoparticles produced by both methods had an average particle size of 6 nm, as seen in Figure 19. However, the nanoparticles often agglomerated to form nanoparticle chains as seen in Figures 20 and 21. The nanoparticle chains produced without the rinsing process were connected with long platinum bridges while the nanoparticle chains produced by with the rinsing process were connected by much shorter platinum bridges. Although the particle sizes were similar, the copper to platinum ratio was different for the two methods. Catalyst without rinsing consisted of



more platinum than copper while catalyst synthesized using the rinsing process consisted of more copper than platinum.

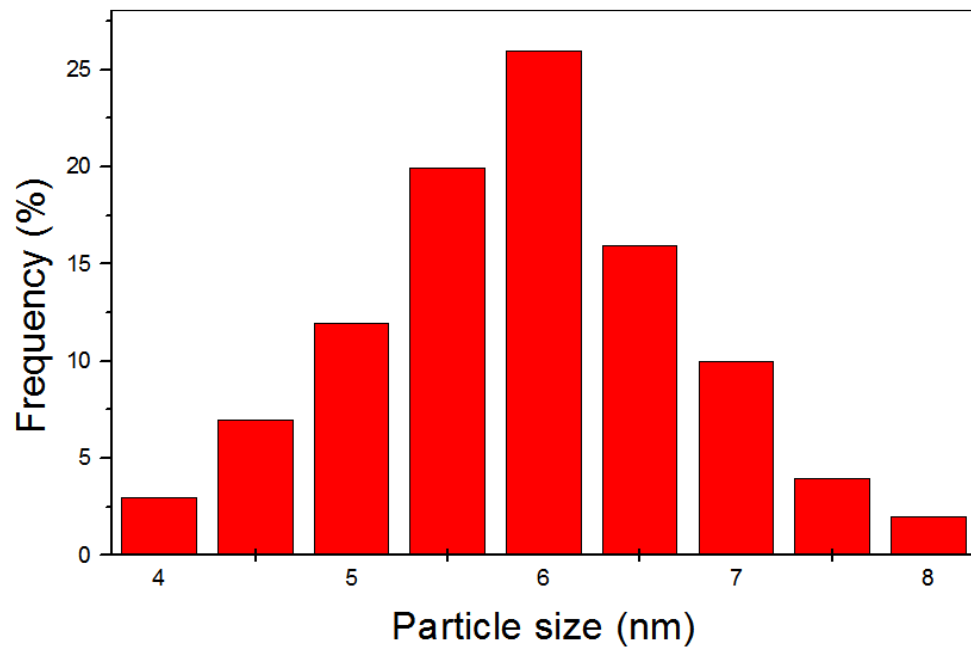


Figure 19 Nanoparticle size distribution of both catalysts

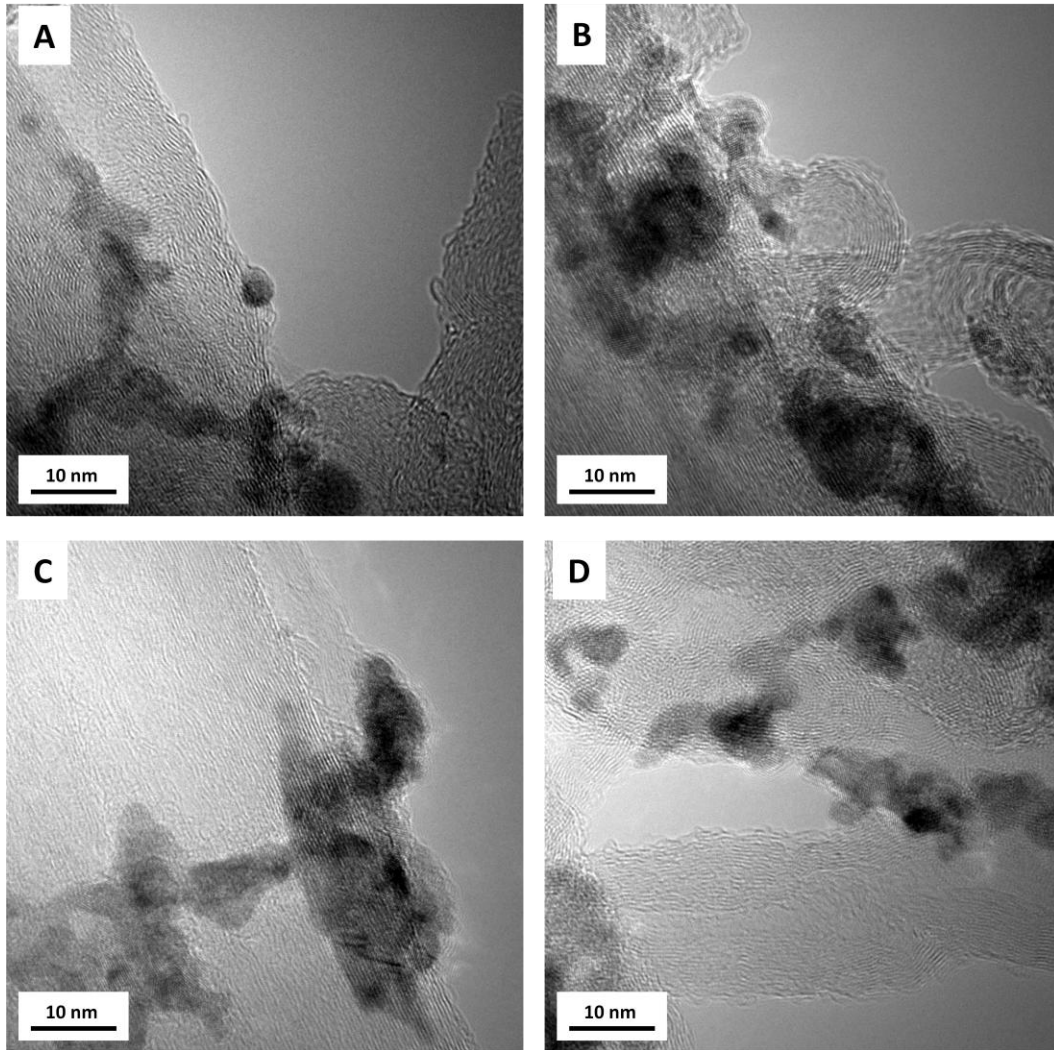


Figure 20 TEM images of core-shell catalyst produced without rinsing showing agglomerated particles

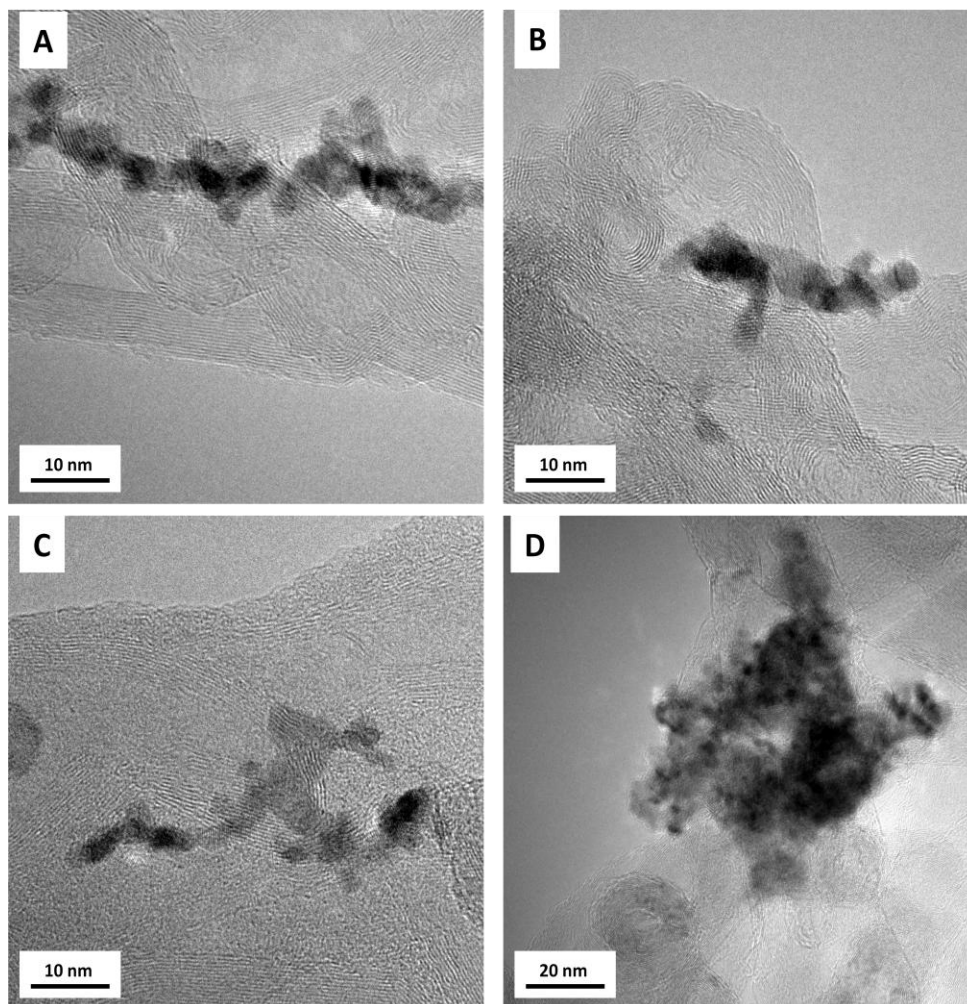


Figure 21 TEM images of core-shell catalyst produced with rinsing showing agglomerated particles

As seen in Figures 22 and 23, not all core-shell nanoparticles contained complete platinum shells and some pure platinum nanoparticles were deposited on the surface of the nanotubes. The incomplete shells were likely a result of incomplete galvanic displacement, which after acid treatment leaves gaps in the shell layer due to the removal of copper [41].

As noted by Podlovchenko *et. al.*, the formation of two-dimensional platinum monolayers and three-dimensional platinum colloids result from

galvanic displacement [40]. It is very likely that the platinum colloids were formed during the galvanic displacement reaction. This occurred much more often in catalyst without using the rinsing method than in catalyst that had been rinsed.

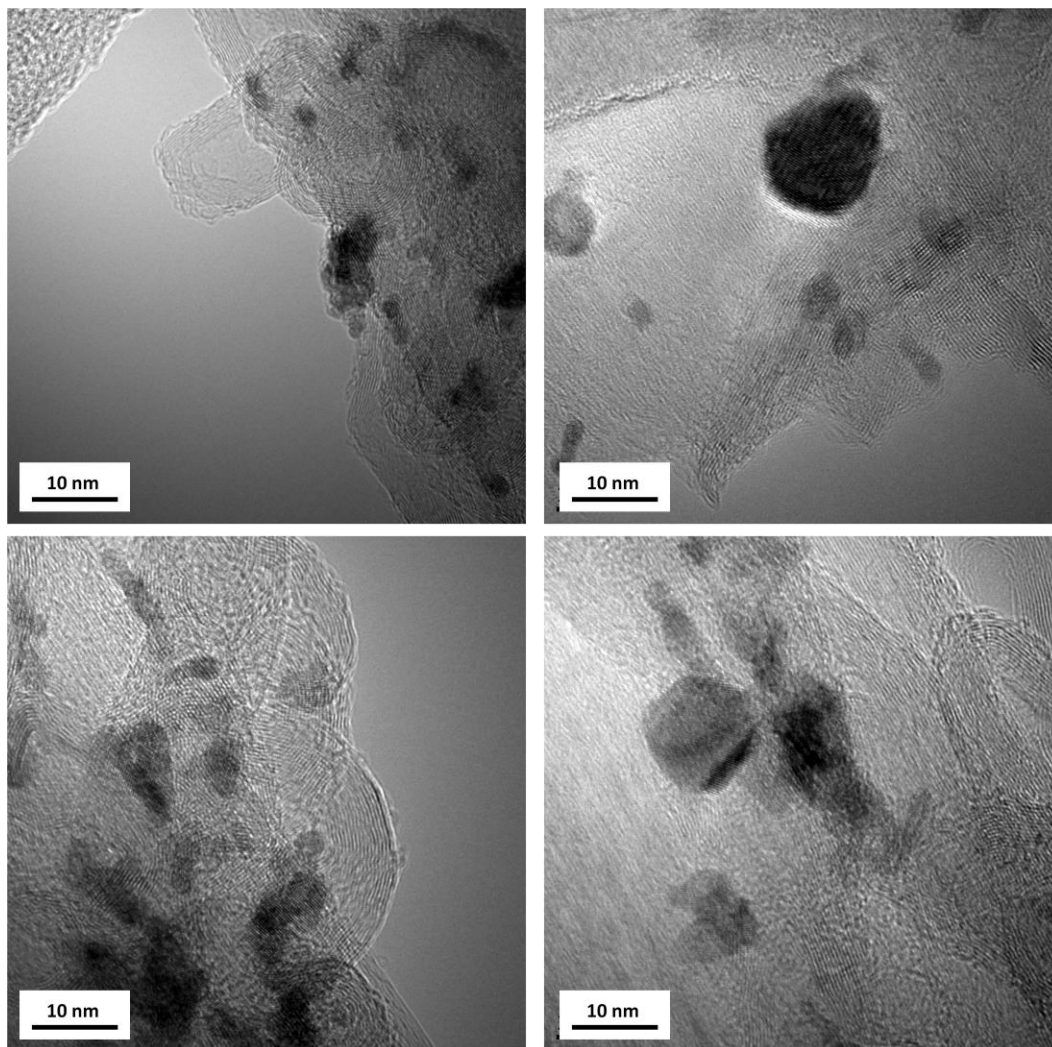


Figure 22 Platinum and copper particles in catalyst produced without rinsing (copper are dark, platinum are light)

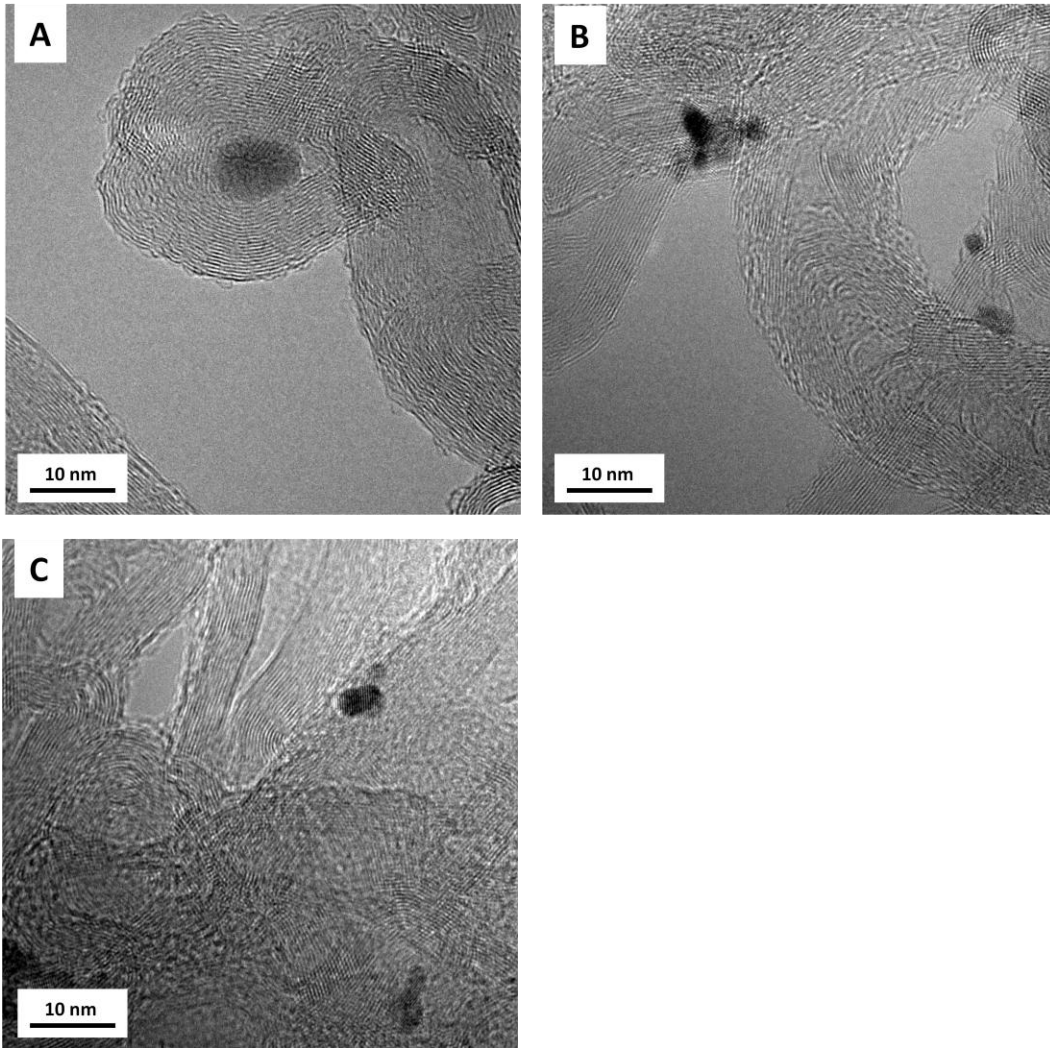


Figure 23 Platinum and copper particles in catalyst produced with rinsing (copper are dark, platinum are light)

It should be noted that the high Molarity sulfuric acid treatment caused defects in the MWCNT structure. Shortening and curling of the MWCNTs, characteristic signs of defects caused by exposure to a strong acid can be seen in Figure 18 A [29].

## Chapter 5

### TWO-PHASE SURFACTANT METHOD

#### 5.1 Experimental details

##### 5.1.1 Fabrication methodology

A novel catalyst synthesis process produced by Lin. *et. al.* was investigated in previous research. This process was modified to determine if dodecanethiol surfactant material could be used to control particle size and distribution during catalyst synthesis. This process utilized a two-phase (water-toluene) solution to determine if copper ions in water would transfer phase into organic medium during reduction. Platinum Pt<sup>4+</sup> ions were extracted using an extraction method produced by Liu *et. al.* then were drop-wise added to the solution to allow for galvanic displacement [47].

##### 5.1.2 Functionalization of carbon nanotubes

In order to improve the wetting characteristics of the MWCNTs, the nanotubes were functionalized with CA to produce hydroxyl (OH<sup>-</sup>) and carboxyl (COOH<sup>-</sup>) groups on the nanotube surface. A 0.9 M solution of citric acid was prepared by adding 500 mg citric acid salt in 1.5 mL DI water. The solution was then ultrasonicated for 15 minutes at room temperature. One hundred milligrams of MWCNTs was added to the solution and the solution was magnetically stirred overnight at room temperature. The solution was then filtered and washed repeatedly with warm DI water in a glass frit filter. The MWCNTs were then heated at 350°C in an oven furnace for 30 minutes then allowed to cool to room temperature.

### 5.1.3 Preparation of copper sulfate solution

A 0.04 M copper sulfate solution was prepared by adding 98 mg copper sulfate pentahydrate to a 2 mL 2mM citric acid solution followed by 15 minutes ultrasonication. A separate solution containing 236 mg DDT in 3 mL toluene was then added to the solution. One hundred milligrams CA functionalized MWCNTs were added to the solution and the solution was magnetically stirred for 30 minutes at room temperature under flowing nitrogen gas before reduction.

### 5.1.4 Copper reduction

A 0.2 M sodium borohydride solution was prepared by adding 38 mg sodium borohydride salt to 5 mL DI water followed by 15 minutes ultrasonication at room temperature. The sodium borohydride solution was then drop-wise added to the MWCNTs/CSP solution over a period of four hours at room temperature. The solution was then stirred for an additional 30 minutes then was left without agitation for one hour before observations were made.

### 5.1.5 Filtering and heat treatment

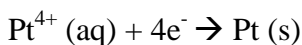
The solution was then filtered and washed with warm DI water in a glass frit filter and was allowed to dry overnight at 70°C in a vacuum oven (vacuum was not used). The dried MWCNTs/Cu was then heat treated at 800°C for one hour in a flowing argon atmosphere.

### 5.1.6 Galvanic displacement

After heat treatment, the dried MWCNTs/Cu catalyst powder was dispersed in a 5mL ethanol solution. A 22 mM solution of chloroplatinic acid was

prepared by adding 27 mg chloroplatinic acid salt to 2 mL ethanol and 1 mL DI water followed by 15 minutes ultrasonication.

The solution was then drop-wise added to the MWCNTs/ Cu solution at room temperature over a two hour period. During this time, a galvanic displacement reaction was to occur between copper nanoparticles and platinum ions ( $\text{Pt}^{4+}$ ) to replace the outer layer of the copper nanoparticles with Pt metal in the following reaction:



Another method was also tried using an ion extraction method produced by Liu, *et. al* [47]. In this method, the MWCNTs/Cu catalyst powder was dispersed in 3mL toluene. A 22 mM solution of chloroplatinic acid was prepared by adding 27 mg chloroplatinic acid salt to 2 mL ethanol and 1 mL DI water followed by 15 minutes ultrasonication. A 0.1 M tetraoctylammonium bromide (ToAB) solution was prepared by adding 164 mg ToAB in 3 mL toluene followed by 15 minutes ultrasonication. The two solutions were then mixed together then magnetically stirred for 30 minutes at room temperature. During this time, the phase transfer catalyst, ToAB, extracted the  $\text{Pt}^{4+}$  ions from the aqueous phase and transferred them to the organic phase, leaving only  $\text{Pt}^{4+}$  ions in the organic layer [47]. The  $\text{Pt}^{4+}$  rich organic layer was then extracted and drop-wise added to the MWCNTs/Cu solution over period of two hours.



#### 5.1.7 Filtering and washing

After the drop-wise addition of platinum, the solution was filtered and washed repeatedly using warm DI water in a glass frit filter then dried overnight at 70°C in a vacuum oven.

#### 5.1.8 Acid treatment

After heat treatment, the MWCNTs/Pt@Cu catalyst powder was added to a 10 mL 9 M sulfuric acid treatment. The mixture was stirred for six hours then the powder was filtered and washed repeatedly with warm DI water. The purpose of the acid treatment was to remove excess copper which had not reacted with platinum [41]. The sulfuric acid dissolves the un-reacted copper, removing copper from the particle shell and also removing un-reacted copper nanoparticles.

#### 5.1.9 Cyclic voltammetry activation and fuel cell testing

Cyclic voltammetry activation and de-alloying was conducted as described in section 3.6 of chapter 3. Fuel cell testing was also conducted according to section 3.6 of chapter 3.

#### 5.1.10 Summary of process steps

A flow chart diagram of the process steps is shown in Figure 24.

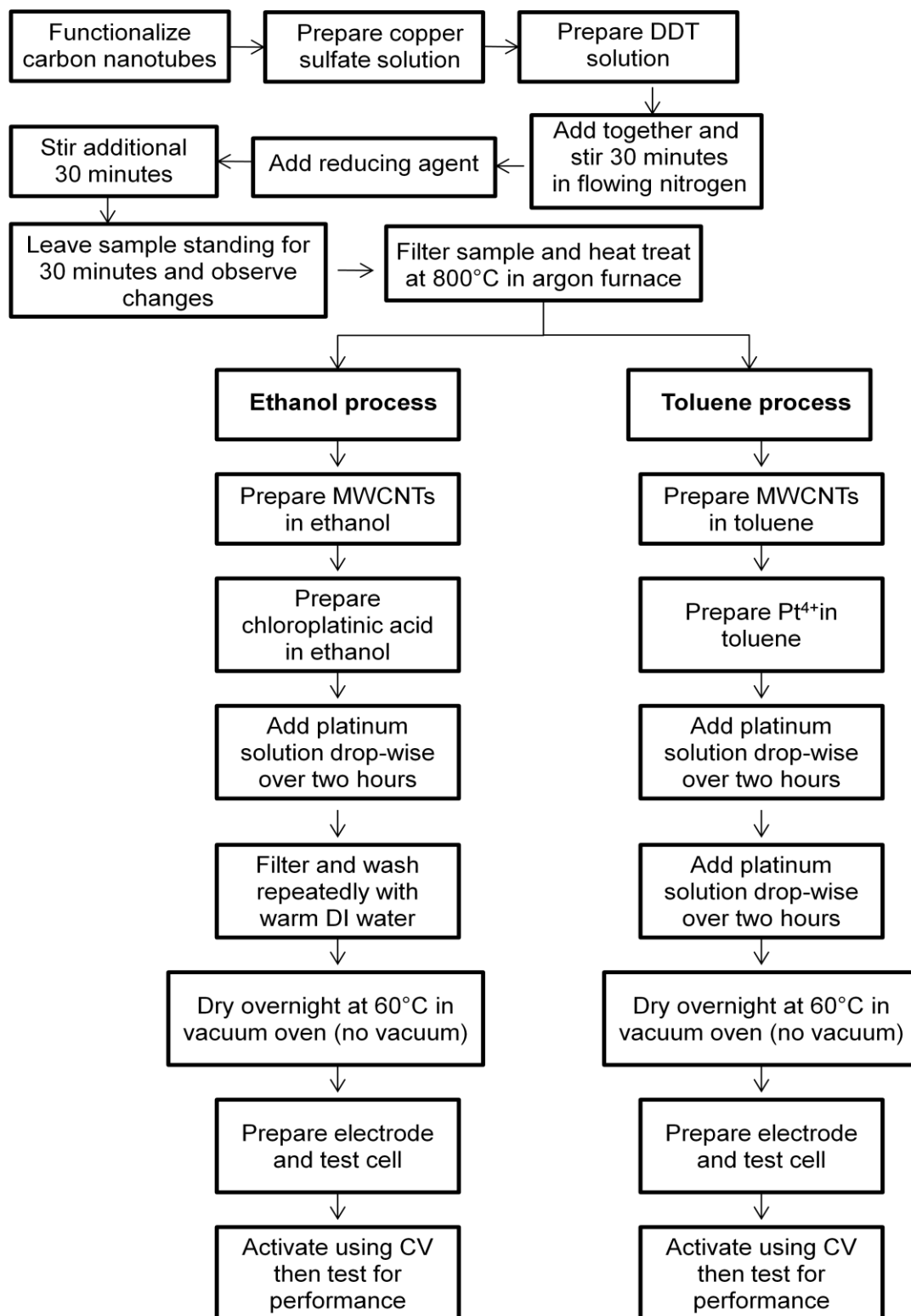






Figure 24 Flow chart diagram of process steps

### 5.1.11 Theoretical nanoparticle structure

-  Cu nanoparticle (A and B)
-  Pt@Cu nanoparticle (C)
-  Carbon molecule (A)
-  Sulfur molecule (A)

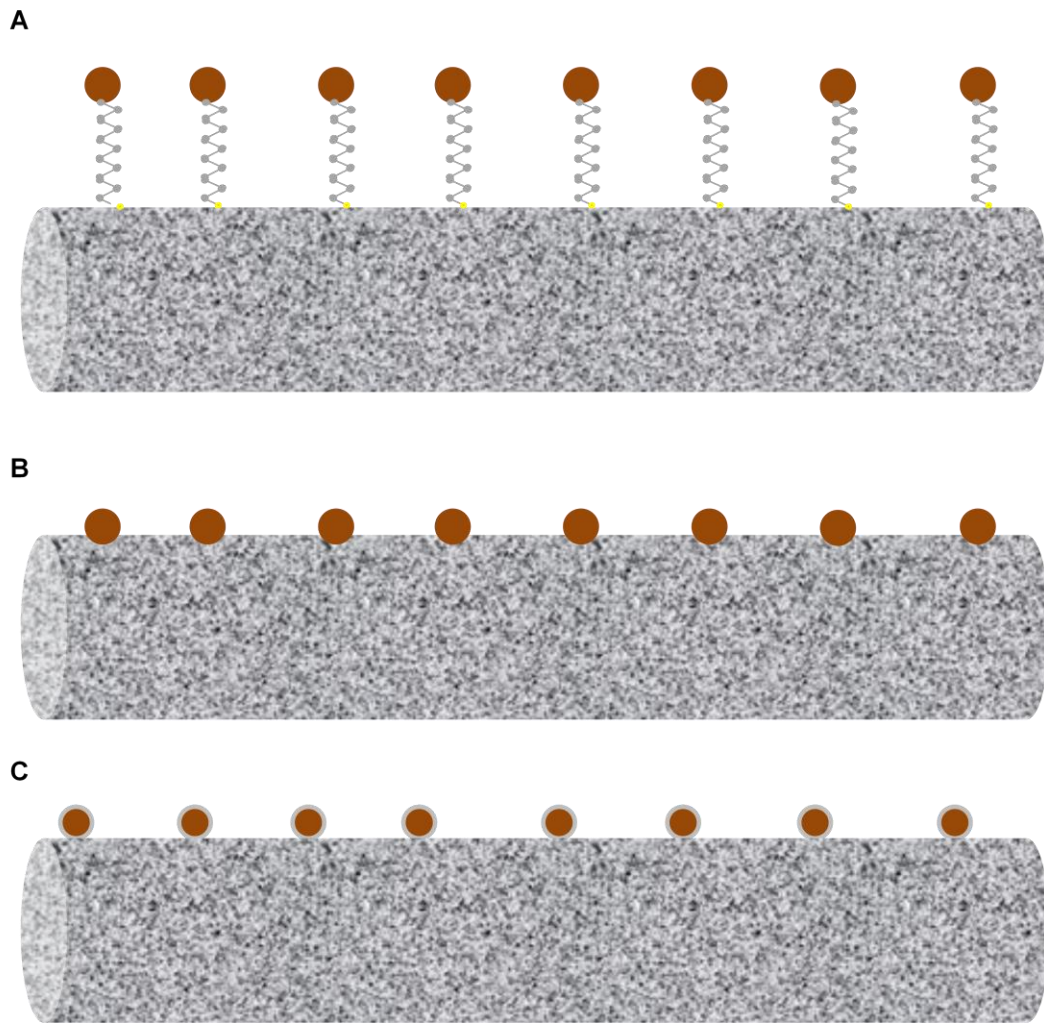


Figure 25 Theoretical nanoparticle structure on MWCNT A) after reduction B) after heat treatment and C) after galvanic displacement

## 5.2 Results and discussion

### 5.2.1 Chemical reduction

It was determined that copper metal ions do not change phase from aqueous phase to organic phase during reduction. This is evident by the blue color of the aqueous solution, indicating copper sulfate was still present after adding the reducing agent. As seen in Figure 26 A, the MWCNTs remain in the organic layer with exception of a cluster attached to the magnet. The aqueous layer was very blue, indicating the presence of copper sulfate. The blue copper sulfate can easily be seen in Figure 26 B.

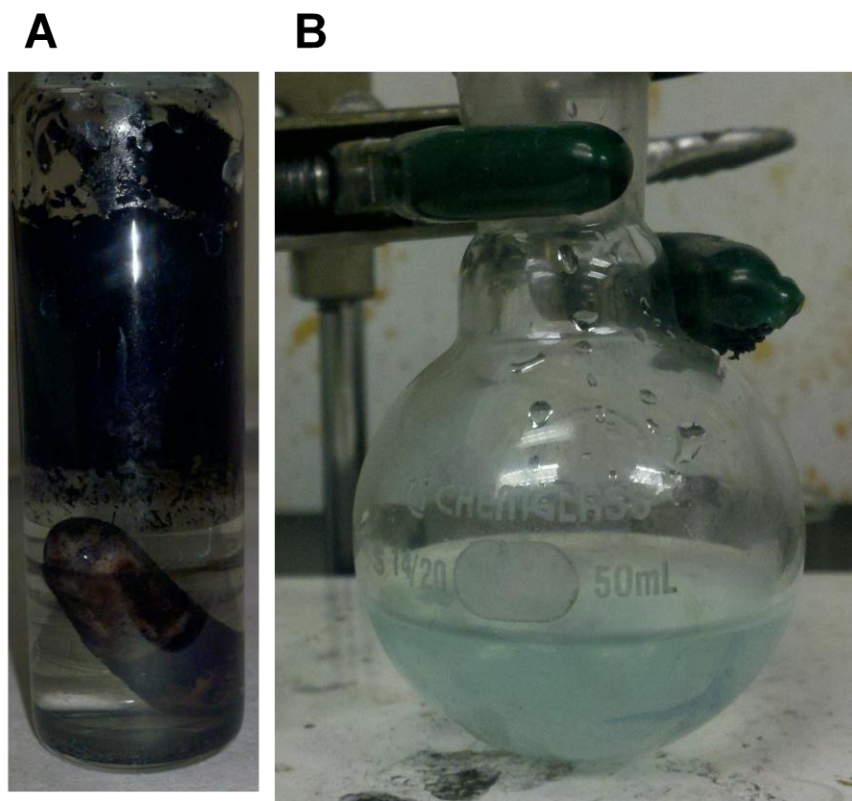


Figure 26 A) sample after copper reduction B) copper sulfate in filter water

### 5.2.2 Galvanic displacement

As seen in Figure 27 A and B, platinum was present in the filter water indicating a galvanic displacement reaction had not occurred. Since there was not any copper present on the MWCNTs for the platinum to form an ion exchange reaction with, it could not be concluded whether galvanic displacement could occur in ethanol and toluene solvents.

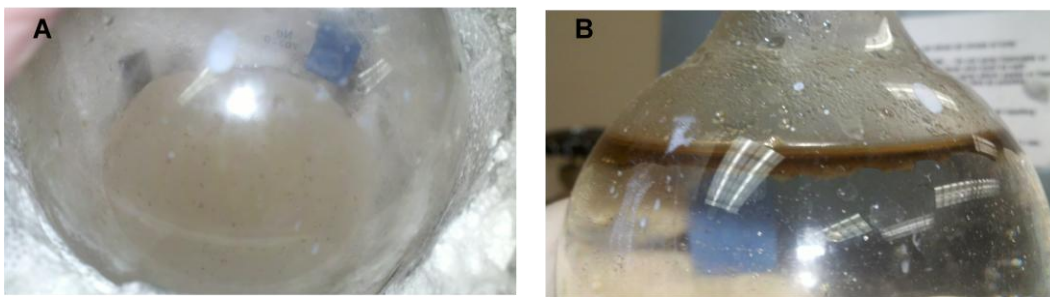


Figure 27 Filter water after galvanic displacement for A) ethanol process

B) toluene process

### 5.2.3 Fuel cell output

The fuel cell output is shown in Figure 28. Even after 100 CV cycles, the open circuit voltage did not exceed 0.7 V and remained around 0.55 V. The cell could not produce any current; even a small load of 100 mA shorted the cell. This poor performance proved that platinum was not on the surface of the MWCNT support. With the results of these experiments as well as other two-phase surfactant experiments not discussed, it has been concluded that dodecanethiol is not a sufficient surfactant material for synthesis of MWCNT/Pt@Cu catalyst.

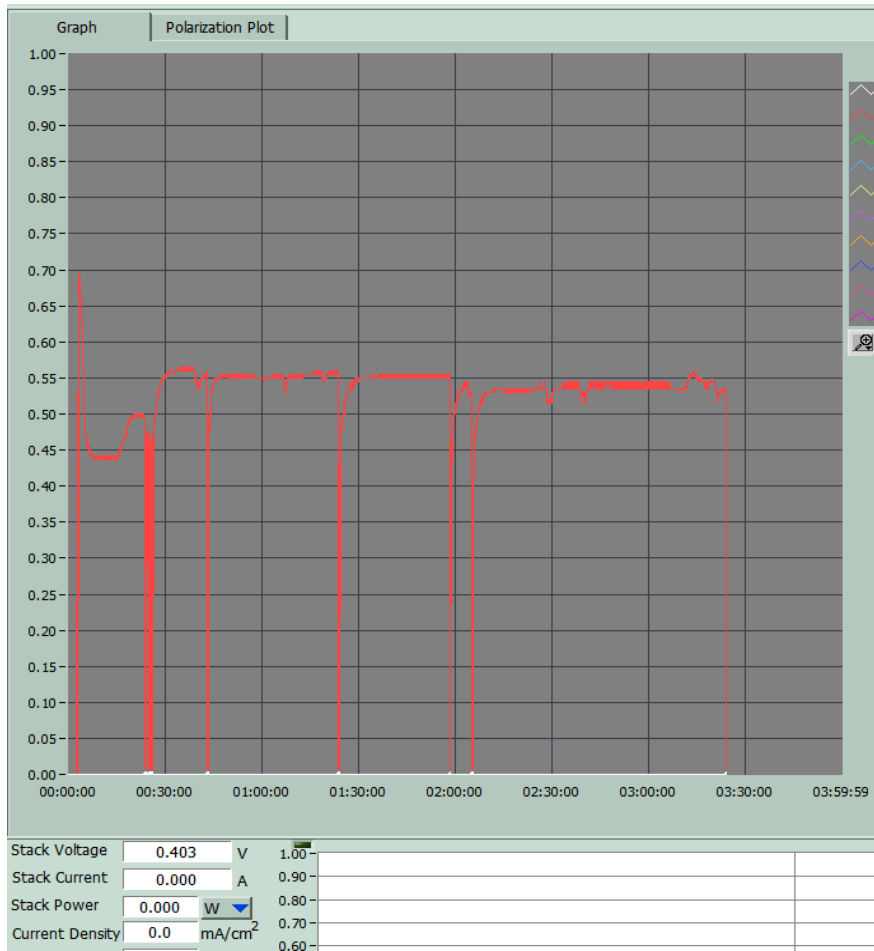


Figure 28 Fuel cell output

## Chapter 6

### SINGLE-PHASE SURFACTANT METHOD

#### 6.1 Experimental details

##### 6.1.1 Fabrication methodology

Sodium dodecyl sulfate was used as a surfactant for MWCNTs/Pt@Cu nanocatalyst synthesis. The SDS served both as a surfactant which would help draw  $\text{Cu}^{2+}$  ions to the surface of the MWCNT for controlled reduction and also as dispersion agent for the MWCNTs by capping the nanotubes with negatively charged heads which would repel other nanotubes. Unlike dodecanethiol, SDS is a water-soluble surfactant, so the process was completed with a single-phase solution.

##### 6.1.2 Functionalization of carbon nanotubes

In order to improve the wetting characteristics of the nanotubes, the pristine MWCNTs were mixed with an 85 mM SDS solution. The SDS solution was prepared by adding 193 mg SDS to 10 mL DI water followed by 15 minutes of ultrasonication. Fifty milligrams of pristine MWCNTs were then added to the solution followed by three hours of ultrasonication. The solution was then heated at 250°C for 40 minutes in an oven furnace.

During functionalization, the hydrophilic tails of the SDS micelles attached to the surface of the carbon nanotube while the hydrophobic heads repelled other nanotubes, allowing the MWCNTs to be individually dispersed in water.

### 6.1.3 Preparation of copper sulfate solution

A 0.02 M copper sulfate solution was obtained by adding 49 mg CSP to a 10 mL 2mM citric acid solution followed by 15 minutes ultrasonication. The functionalized MWCNTs obtained after heating were then added to the copper sulfate solution and the solution was ultrasonicated for 5 minutes followed by 30 minutes magnetic stirring under flowing nitrogen.

### 6.1.4 Copper reduction

An 80 mM sodium borohydride solution was prepared by adding 15 mg sodium borohydride salt to 6 mL DI water followed by ultrasonication for 15 minutes. The solution was then drop-wise added to the copper sulfate/MWCNTs solution over a two hour period at room temperature. After all the solution was added, the solution was stirred for an additional 30 minutes then was left sitting for 30 minutes without agitation.

### 6.1.5 Rinsing with DI water

After the MWCNTs settled to the bottom of the vial, the aqueous solvent was removed from the vial using a 20 gauge needle syringe, leaving only the MWCNTs/Cu catalyst in the vial. Immediately after, 8 mL DI water and then the solution was stirred for 15 minutes. The entire process was conducted under flowing nitrogen to prevent oxidation of the copper nanoparticles.

### 6.1.6 Galvanic displacement

A 0.5 mM solution of chloroplatinic acid was obtained by adding 6 mg chloroplatinic acid hexahydrate salt to 3 mL DI water followed by 15 minutes ultrasonication. The solution was then added drop-wise to the reduced copper



sulfate/MWCNTs solution over a period of two hours at room temperature under flowing nitrogen. After all solution had been added, it was stirred for an additional thirty minutes.

#### 6.1.7 Filtering and heating

After the additional stirring, the solution was filtered and washed repeatedly using warm DI water in a glass frit filter, then dried overnight at 70°C in a vacuum oven. The solid MWCNTs/Pt@Cu powder was then extracted and heated in a tubular furnace at 800°C for one hour in a flowing argon atmosphere.

#### 6.1.8 Acid treatment

After heat treatment, the MWCNTs/Pt@Cu catalyst powder was added to a 10 mL 9 M sulfuric acid solution. The mixture was stirred for six hours at room temperature then was filtered and washed repeatedly with warm DI water. The catalyst mixture was then dried overnight at 70°C in a vacuum oven (vacuum not used).

#### 6.1.9 Cyclic voltammetry and fuel cell testing

Cyclic voltammetry activation and de-alloying was conducted as described in section 3.6 of chapter 3. Fuel cell testing was also conducted according to section 3.6 of chapter 3.

6.1.10 Summary of process steps

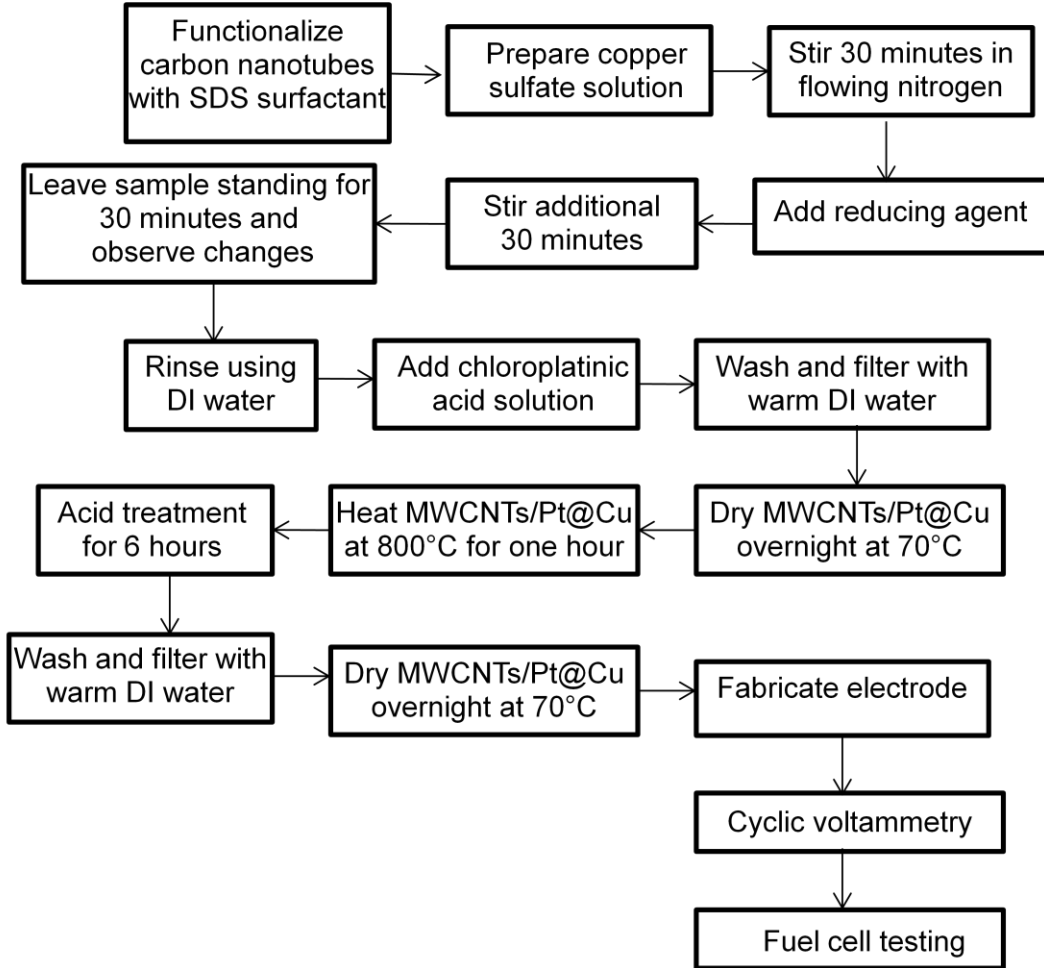






Figure 29 Flow chart diagram of process steps

### 6.1.11 Theoretical nanoparticle structure

-  Cu nanoparticle (A)
-  Pt@Cu nanoparticle (B and C)
-  Sulfate head (A and B)
-  SDS chain (A and B)

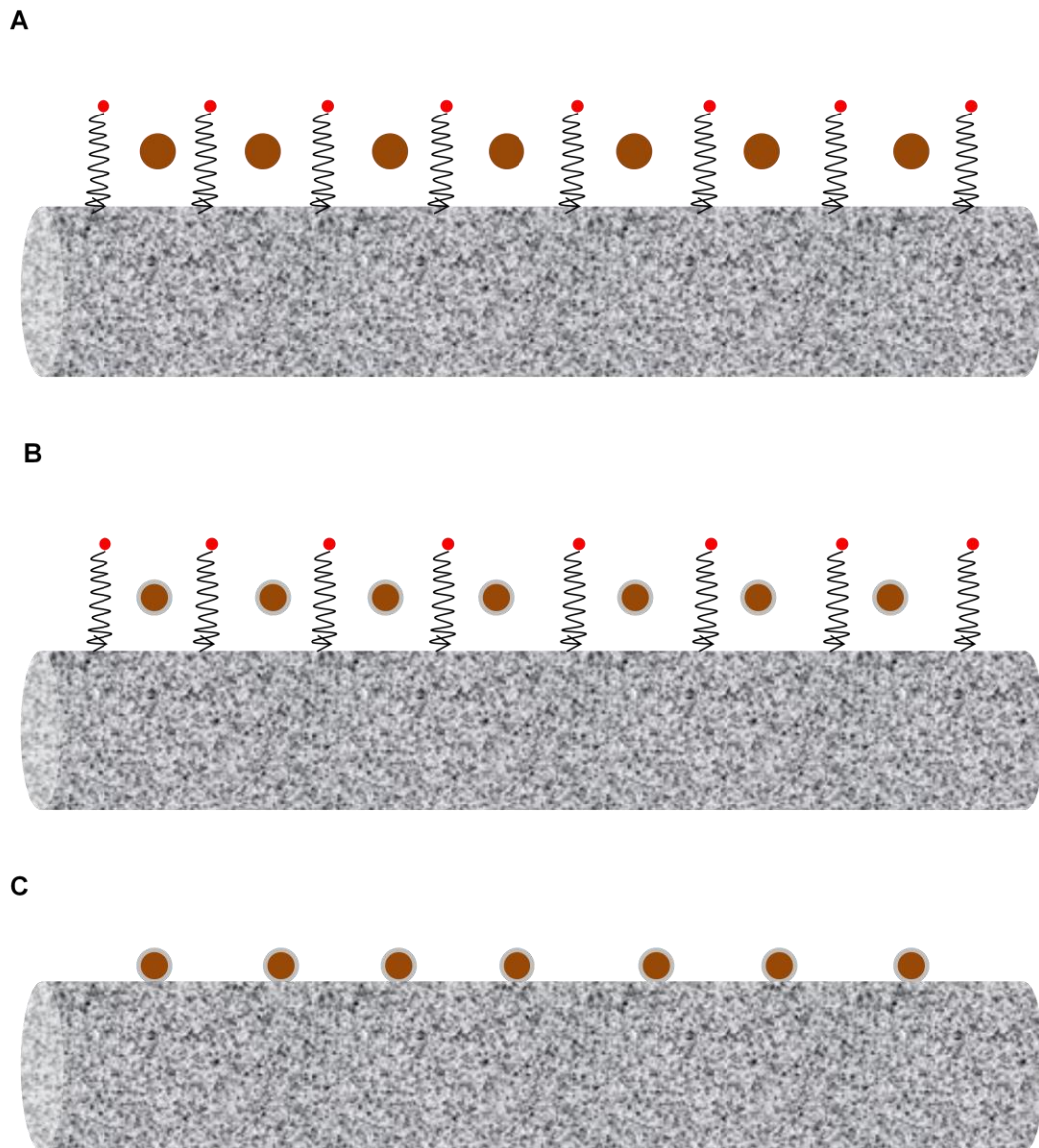


Figure 30 Theoretical nanoparticle structure A) after reduction, B) after galvanic displacement, C) after heat treatment

## 6.2 Results and discussion

### 6.2.1 Chemical processing

After copper reduction, the liquid layer of the sample was clear, indicating a complete reduction reaction. There were not any copper films in the liquid and no visible oxidation was observed. After adding the chloroplatinic acid, the liquid layer was clear, indicating the platinum was used, but galvanic displacement may not have occurred. Figure 31 shows the sample after reduction.



After reduction



After galvanic displacement

Figure 31 SDS sample after reduction and galvanic displacement

### 6.2.2 Fuel cell output

The MWCNTs/Pt@Cu catalyst synthesized using SDS surfactant was shown to be a very ineffective catalyst. The catalyst did not produce any voltage

in the cell, and even after 100 CV cycles, the cell only reached a maximum of 0.1 V and could not hold any current. Due to very low OCV) an EG&G PARSTAT-2273 potentiostat–galvanostat was used drive the open circuit voltage above its normal value. Even with the use of the PARSTAT, the cell voltage would quickly drop down to a short as soon as current was drawn. The fuel cell voltage characteristics are shown in Figure 32.

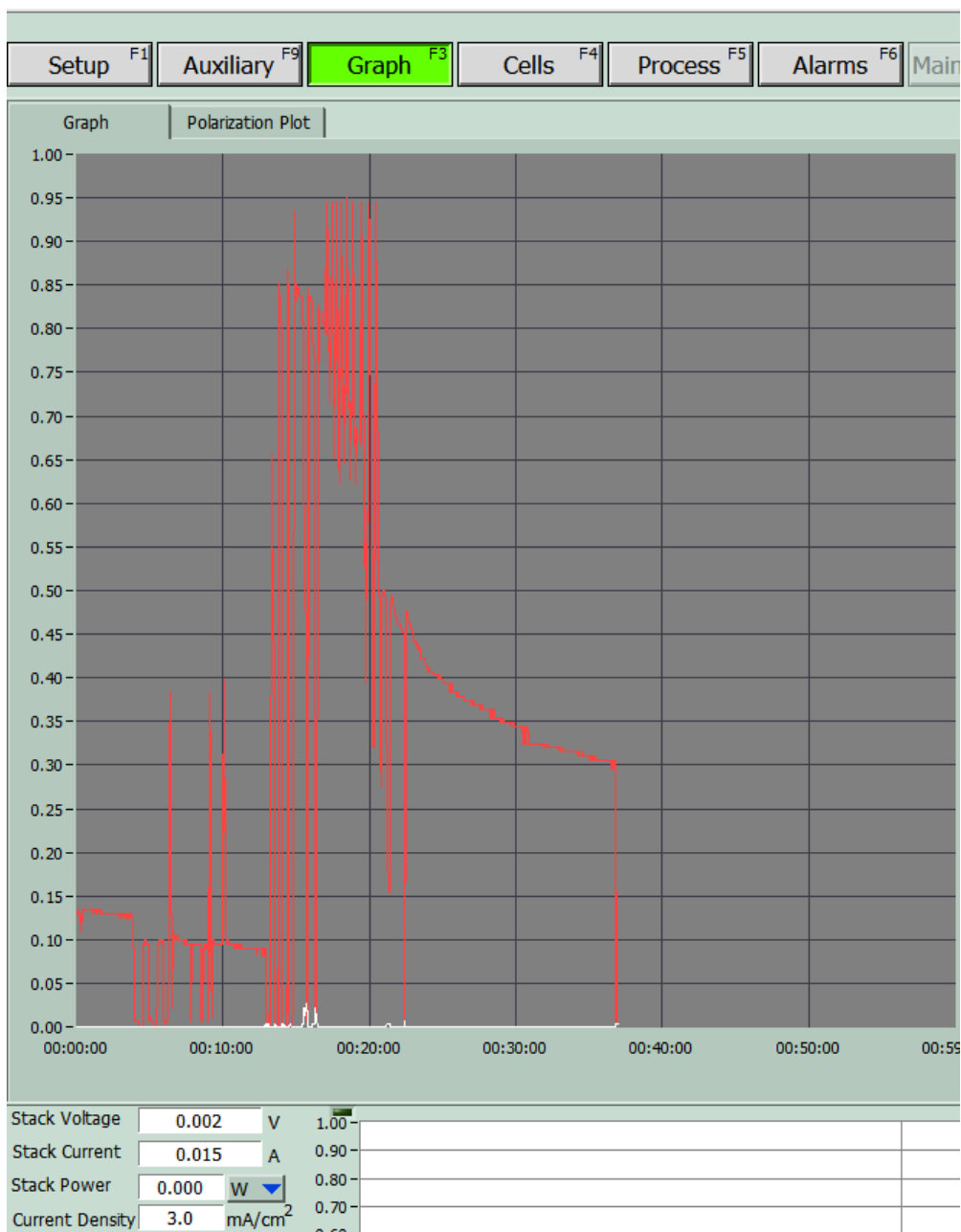


Figure 32 SDS catalyst fuel cell voltage characteristics

Based on the fuel cell output, the single-phase surfactant synthesis method was not successful. It is evident that this method does not work with the current concentration of reducing agent and concentration of SDS. Possible causes for failure include failure of SDS surfactant to disperse copper nanoparticles on the

surface of the MWCNTs and SDS interference with galvanic displacement. It is possible that the SDS micelles do not attract  $\text{Cu}^{2+}$  ions to the surface of the MWCNT and that copper nanoparticles do not form on the MWCNT. It is also possible that the SDS micelles interfere with the galvanic displacement process by creating resistance between copper nanoparticles and  $\text{Pt}^{4+}$  ions. The micelles may in fact block the  $\text{Pt}^{4+}$  ions from reaching the copper nanoparticles. It is also possible that the negatively charged sulfate head of the SDS micelle attracts the  $\text{Pt}^{4+}$  ions, keeping them from reaching the copper nanoparticles.

Only the SDS concentration used by Lin, *et. al.*, was studied [18]. It is possible that SDS could be a useful surfactant for Pt@Cu nanocatalyst synthesis, however, no conditions have been found for successful results. Other preparation methods including heat treatment before galvanic displacement, rinsing through the use of a centrifuge, and dispersing of chloroplatinic acid in ethanol were investigated but not included in this thesis. It is possible that SDS could be used with other copper sources to produce MWCNTS/Pt@Cu, however, only synthesis with copper sulfate pentahydrate was used.

## Chapter 7

### CONCLUSION

#### 7.1 Overview

Of the three Pt@Cu core-shell nanocatalyst synthesis methods, the direct deposition method was successful while the synthesis methods that used surfactants were unsuccessful. Using the direct deposition method, a highly functional Pt@Cu core-shell binary catalyst on multi-walled carbon nanotubes support was developed. The core-shell binary catalyst which was rinsed before galvanic displacement obtained high power capability, producing a peak power density of  $618 \text{ mW.cm}^{-2}$  which is 13 percent greater than that of commercial platinum-carbon catalyst with similar platinum loading. Transmission electron microscopy revealed platinum-copper core-shell binary nanoparticles with platinum shells and platinum-copper alloy cores dispersed on the surface of multi-walled carbon nanotubes. The step of rinsing before galvanic displacement was shown to be essential as the platinum ions were more efficiently utilized in solution which had been rinsed of remaining reducing agent.

While sodium borohydride was shown to be an effective reducing agent for reducing  $\text{Cu}^{2+}$  ions in copper sulfate solution, sodium formate was shown to be ineffective for copper reduction, even at relatively high Molarity of up to 10 M. Additionally, the amount of sodium borohydride added was shown to be a critical parameter in nanoparticle synthesis.

Catalyst synthesis using the organic surfactant, dodecanethiol, was shown to be unsuccessful due to the inability of copper ions to transfer between solvents



during reduction. Fuel cell testing revealed the presence of material on the carbon nanotubes, but very little platinum, if any was present. Synthesis using the water-soluble surfactant, sodium dodecyl sulfate was shown to be unsuccessful with the parameters described in this thesis. It is unknown exactly why synthesis was unsuccessful; however, possible causes have been discussed in this thesis.

## 7.2 Future recommendations

The platinum catalyst material used in low temperature fuel cells currently makes up roughly half the cost of a fuel cell system. Any catalyst research focused in reducing or eliminating the fuel cell's dependency on platinum is greatly encouraged. The three synthesis techniques investigated in this work were the first core-shell nanocatalyst synthesis techniques investigated in the Arizona State University Fuel Cell Laboratory. There are still many different synthesis processes that can be investigated. Different copper sources such as copper (II) chloride dehydrate, copper (II) acetate, and copper (II) carbonate can be used for deposition in substitution for copper (II) sulfate. A phase transfer catalyst will likely be necessary if a two-phase method is used. In addition, additional processes using sodium dodecyl sulfate can be investigated. Synthesis using polymer based materials such as polyethylene glycol and polyvinylpyrrolidone can also be investigated.

## REFERENCES

- [1] University of Delaware, "Fuel Cell Research Lab," *Research Groups*, [online]. Accessed Nov. 13, 2011. Available: [http://www.me.udel.edu/research\\_groups/prasad/research/overview.html](http://www.me.udel.edu/research_groups/prasad/research/overview.html)
- [2] Y. Shao, J. Liu, Y. Wang, and Y. Lin, "Novel catalyst support materials for PEM fuel cells: current status and future prospects," *J. Mater. Chem.*, 2009, vol. 19, pp. 46–59.
- [3] D. Gross, "Fuel Cells: 170 years of technology development - and space age experience," *Cleantech Magazine*, [online]. Accessed: Sept.18, 2011. Available:<http://www.cleantechinvestor.com/portal/fuel-cells/6455-fuel-cell-history.html>.
- [4] B. Cunningham and D. Baird, "The development of economical bipolar plates for fuel cells," *J. Mater. Chem.*, 2006, vol. 16, pp. 4385–4388.
- [5] D. Gross, "Fuel Cells: 170 years of technology development - and space age experience," *Cleantech Magazine*, [online]. Accessed: Sept. 18, 2011. Available: <http://www.cleantechinvestor.com/portal/fuel-cells/6455-fuel-cell-history.html>
- [6] [University of Cambridge, "Proton exchange membrane fuel cells (PEMFCs)," *Dissemination of IT for the Promotion of Materials Science (DoITPoMS)*, [online]. Accessed Nov. 13, 2011. Available: [http://www.doitpoms.ac.uk/tlplib/fuel-cells/low\\_temp\\_pem.php](http://www.doitpoms.ac.uk/tlplib/fuel-cells/low_temp_pem.php)
- [7] R. Othman, A. Dicks, Z. Zhu, "Non precious metal catalysts for the PEM fuel cell cathode," *International Journal of Hydrogen Energy*, Vol. 37, Issue 1, January 2012, Pages 357-372.
- [8] S.A. Grigoriev, E.K. Lyutikova, S. Martemianov, V.N. Fateev, "On the possibility of replacement of Pt by Pd in a hydrogen electrode of PEM fuel cells," *International Journal of Hydrogen Energy*, Vol. 32, Issue 17, December 2007, Pages 4438-4442.
- [9] G.Liu, X. Li, P. Ganesan, B.N. Popov, "Development of non-precious metal oxygen-reduction catalysts for PEM fuel cells based on N-doped ordered porous carbon," *Applied Catalysis B: Environmental*, Vol.93, Issues 1–2, 25 November 2009, Pages 156-165.

- [10] N. Ramaswamy and S. Mukerjee, "Fundamental Mechanistic Understanding of Electrocatalysis of Oxygen Reduction on Pt and Non-Pt Surfaces: Acid versus Alkaline Media," *Advances in Physical Chemistry*, vol. 2012, Article ID 491604, 17 pages, 2012.
- [11] C. Song and J. Zhang, "Electrocatalytic Oxygen Reduction Reaction," *PEM Fuel Cell Electrocatalysts and Catalyst Layers: Fundamentals and Applications*, 1<sup>st</sup> edition, Guildford, Surrey, U.K., Springer-Verlag London Ltd, 2008, ch. 2, pp. 92.
- [12] R.A. Messenger and J. Venture, "Chemical Corrosion and Ultraviolet Degradation , *Photovoltaic Systems Engineering*, 3<sup>rd</sup> edition, Boca Raton, FL., CRC Press, 2010, Ch. 5, pp.173.
- [13] Y. Shao, G. Yin, Y. Gao, "Understanding and approaches for the durability issues of Pt-based catalysts for PEM fuel cell," *Journal of Power Sources*, Vol. 171, Issue 2, 27 September 2007, pp. 558-566.
- [14] J. Zhang, *PEM Fuel Cell Electrocatalysts and Catalyst Layers: Fundamentals and Applications*, London: Springer-Verlag, 2008, pp. 13-16.
- [15] J.F. Lin, V. Kamavaram, A.M. Kannan, "Synthesis and characterization of CNT supported Pt nanocatalyst for PEMFC," *Journal of Power Sources*, Vol. 195, Issue 2, 15 January 2010, pp. 466-470.
- [16] S. Trasatti and O.A. Petrii, "Real Surface Area Measurements in Electrochemistry," *Pure & Appl.Chem.*, Vol. 63, No. 5, pp. 71 1-734, 1991.
- [17] R. Borup, J. Davey, D. Wood, F. Garzon, and M. Inbody, "PEM Fuel Cell Durability," *DOE Hydrogen Program*, FY 2005 Progress Report, 2005, [online]. Accessed October 4, 2011.  
Available:  
[http://www.hydrogen.energy.gov/pdfs/progress05/vii\\_i\\_3\\_borup.pdf](http://www.hydrogen.energy.gov/pdfs/progress05/vii_i_3_borup.pdf)
- [18] J.F. Lin, C.W. Mason, A. Adame, X. Liu, X.H. Peng, and A.M.Kannan, "Synthesis of Pt nanocatalyst with micelle-encapsulated multi-walled carbon nanotubes as support for proton exchange membrane fuel cells," *Electrochimica Acta*, Vol. 55, Issue 22, 1 September 2010, Pages 6496-6500.
- [19] M. Mathias, "Electrification Technology and the Future of the Automobile," *2010 Advanced Energy Conference*, Nov. 8, 2010. [online]. Accessed October 4, 2011. Available:  
[http://www.aertc.org/conference2010/speakers/AEC%202010%20Session%](http://www.aertc.org/conference2010/speakers/AEC%202010%20Session%20)

- [20] Innovation Energy UK Ltd, "Fuel Cell," *ieukltd.com*, 2010. [online].  
Accessed October 4, 2011.  
Available: [http://ieukltd.com/index.php?p=1\\_4\\_Technology](http://ieukltd.com/index.php?p=1_4_Technology)
- [21] R. Jain and B. Mandal, "Studies on Ideal and Actual Efficiency of Solar Polymer Electrolyte Fuel Cell," *AltEnergyMag*, Feb. 2007. [online].  
Accessed October 4, 2011. Available:  
[http://www.altenergymag.com/emagazine.php?issue\\_number=07.02.01&article=solar\\_polymer](http://www.altenergymag.com/emagazine.php?issue_number=07.02.01&article=solar_polymer)
- [22] Y. Wang, S. Song, V. Maragou, P.K.. Shen, P. Tsiakaras, "High surface area tungsten carbide microspheres as effective Pt catalyst support for oxygen reduction reaction," *Applied Catalysis B: Environmental*, Vol. 89, Issues 1–2, 3 July 2009, pp. 223-228.
- [23] C.K. Achararya, W. Li, Z. Liu, G. Kwon, C.H. Turner, A.M. Lane, D. Nikles, T. Klein, M. Weaver," "Effect of boron doping in the carbon support on platinum nanoparticles and carbon corrosion," *Journal of Power Sources*, Vol. 192, Issue 2, 15 July 2009, pp. 324-329.
- [24] L. Calvillo, M. Gangeri, S. Perathoner, G. Centi, R. Moliner, M.J. Lazaro, "Effect of the support properties on the preparation and performance of platinum catalysts supported on carbon nanofibers," *Journal of Power Sources*, Vol. 192, Issue 1, 1 July 2009, pp. 144-150.
- [25] S.K. Cui, D.J. Guo, "Highly dispersed Pt nanoparticles immobilized on 1, 4-benzenediamine-modified muil-walled carbon nanotube for methanol oxidation," *Journal of Colloid and Interface Science*, vol. 333 (2009) pp. 300–303.
- [26] M. S. Dresselhaus, G. Dresselhaus, Ph. Avouris (Eds.): *Carbon Nanotubes*, Topics Appl. Phys. 80, 29–53, 2001.
- [27] R. Reilly, "Carbon Nanotubes: Potential Benefits and Risks of Nanotechnology," *Journal of Nuclear Medicine*, Vol. 48, No. 7, July 2007, pp. 1039-1042.
- [28] C.K. Poh, S.Lim, H. Pan, J. Lin, J.Y. Lee, "Citric acid functionalized carbon materials for fuel cell applications," *Journal of Power Sources*, Vol. 176, Issue 1, 21 January 2008, pp. 70-75.

- [29] K. Zhang, H.J. Choi, J.H. Kim, "Preparation and characteristics of electrospun multiwalled carbon nanotube/polyvinylpyrrolidone nanocomposite nanofibers," *J. Nanosci. Nanotechnology*, June 2011, pp. 5446-9.
- [30] M. Burghard, K. Balasubramanian, "Chemically Functionalized Carbon Nanotubes," *Small*, 1: 180–192.(2005) doi: 10.1002/sml.200400118.
- [31] J.F. Lin, A. Adame, A.M. Kannan, "Development of durable platinum nanocatalyst on carbon nanotubes for PEMFCs," *J. Electrochem. Soc.* 157, B846-B851, 2010.
- [32] M. Brust, M. Walker, D. Bethell, D. Schiffrin, R. Whyman, "Synthesis of thiol-derivatised gold nanoparticles in a two-phase liquid-liquid system," *Colloids and Surfaces A: Physicochemical and Engineering Aspects*, Vol. 390, Issues 1–3, 20 October 2011, pp. 149-156.
- [33] E. Castro, R. Salvatierra, W. Schreiner, M. Oliveira, A. Zarbon, "Dodecanethiol-stabilized platinum nanoparticles obtained by a two-phase method: synthesis, characterization, mechanism of formation, and electrocatalytic properties.," *Chem. Mater.*, 2010, 22 (2), pp 360-370.
- [34] Q. Tan, K. Zhang, S. Gu, J. Ren, "Mineralization of surfactant functionalized multi-walled carbon nanotubes (MWNTs) to prepare hydroxyapatite/MWNTs hybrid," *Applied Surface Science*, Vol.255, Issue 15, 15 May 2009, pp. 7036-7039.
- [35] J. Zhang, L. Gao, "Dispersion of multiwall carbon nanotubes by sodium dodecyl sulfate for preparation of modified electrodes toward detecting hydrogen peroxide," *Materials Letters*, Vol. 61, Issue 17, July 2007, pp. 3571-3574.
- [36] C.L. Lee, Y.C. Ju, P.T. Chou, Y.C. Huang, L.C. Kuo, J.C. Oung, "Preparation of Pt nanoparticles on carbon nanotubes and graphite nanofibers via self-regulated reduction of surfactants and their application as electrochemical catalyst, *Electrochemistry Communications*, vol. 7 (2005), pp. 453-458.
- [37] A. Ulman, "Formation and structure of self-assembled monolayers," *Chem. Rev.* 1996, 96, pp. 1533-1554.
- [38] K.C. Pngali, S. Deng, D. Rockstraw, "Direct synthesis of Ru-Ni core-shell nanoparticles by spray-pyrolysis: Effect of temperature and precursor constituent," *Powder Technology*, 183 (2008) pp. 282-289.

- [39] Z.D. Wei, Y.C. Feng, L.L. Liao, Y. Fu, C.X. Sun, Z.G. Shao, P.K. Shen, "Electrochemically synthesized Cu/Pt core-shell catalysts on a porous carbon electrode for polymer electrolyte fuel cells," *Journal of Power Sources*, Vol. 180, Issue 1, 15 May 2008, pp. 84-91.
- [40] B.I. Povlenko, T.D. Gladysheva, A.Y. Filatov, L.V. Yahshina, "Displacement in Synthesizing Pt(Cu) Catalysts with the Core-Shell Structure," *Russian Journal of Electrochemistry*, Vol 46., Num. 10, pp. 1189-1197.
- [41] A. Sarkar and A. Manthiram, "Synthesis of Pt@Cu core-shell nanoparticles by galvanic displacement by Pt<sup>4+</sup> ions and their application as electrocatalysts for oxygen reduction reaction in fuel cells," *J. Phys. Chem., C* 2010, 114, pp 4725-4732.
- [42] S. Alayoglu, A.U. Nilekar, M. M Mavrikakis, B. Eichhorn, "Ru-Pt core-shell nanoparticles oxidation of carbon monoxide in water," *Nature Materials*. April 2008, vol. 7, pp. 333-338.
- [43] G. Glavee, K. Klabunde, C. Sorensen, G. Hadjipanayis, "Borohydride reduction of nickel and copper ions in aqueous and nonaqueous media. Controllable chemistry leading to nanoscale metal and metal boride particles," *Langmuir*, 1994, 10, pp. 4726-4730.
- [44] I. Choi, S.H. Ahn, J.J. Kim, O.H. Kwon, "Preparation of Pt<sub>shell</sub>-Pd<sub>core</sub> nanoparticle with electroless deposition of copper for polymer electrolyte membrane fuel cell," *Applied Catalysis B: Environmental*, Vol. 102, Issues 3-4, 22 February 2011, pp. 608-613.
- [45] N.D. Subramanian, G. Balaji, C.S.S.R. Kumar, J.J. Spivey, "Development of cobalt-copper nanoparticles as catalysts for higher alcohol synthesis from syngas," *Catalysis Today*, Vol. 147, Issue 2, 30 September 2009, pp. 100-106.
- [46] X. Li, J. Liu, W. He, Q. Huang, H. Yang, "Influence of the composition of core-shell Au-Pt nanoparticle electrolysis for the oxygen reduction reaction," *Journal of Colloid and Interface Science*, Vol. 344, Issue 1, 1 April 2010, pp. 132-136.
- [47] X. Liu, R. Villacorta, A. Adame, A.M. Kannan, "Comparison of Pt/MWCNTs nanocatalysts synthesis processes for proton exchange membrane fuel cells," *International Journal of Hydrogen Energy*, Vol. 36, Issue 17, August 2011, pp. 10877-10888.

